ISTANBUL TECHNICAL UNIVERSITY ★ GRADUATE SCHOOL

EXACT SOLITON SOLUTIONS OF CUBIC NONLINEAR SCHRÖDINGER EQUATION WITH A MOMENTUM TERM

M.Sc. THESIS

Haldun Taha UZUNOĞLU

Department of Mathematics Engineering

Mathematics Engineering Programme

DECEMBER 2024

ISTANBUL TECHNICAL UNIVERSITY ★ GRADUATE SCHOOL

EXACT SOLITON SOLUTIONS OF CUBIC NONLINEAR SCHRÖDINGER EQUATION WITH A MOMENTUM TERM

M.Sc. THESIS

Haldun Taha UZUNOĞLU
(509221207)

Department of Mathematics Engineering

Mathematics Engineering Programme

Thesis Advisor: Prof. Dr. İlkay BAKIRTAŞ AKAR

DECEMBER 2024

İSTANBUL TEKNİK ÜNİVERSİTESİ ★ LİSANSÜSTÜ EĞİTİM ENSTİTÜSÜ

MOMENTUM TERİMİ İÇEREN KÜBİK NONLİNEER SCHRÖDINGER DENKLEMİNİN SOLİTON TİPİ ÇÖZÜMLERİ

YÜKSEK LİSANS TEZİ

Haldun Taha UZUNOĞLU
(509221207)

Matematik Mühendisliği Anabilim Dalı

Matematik Mühendisliği Programı

Tez Danışmanı: Prof. Dr. İlkay BAKIRTAŞ AKAR

ARALIK 2024

Haldun Taha UZUNOĞLU, a M.Sc. student of ITU Graduate School 509221207 successfully defended the thesis entitled "EXACT SOLITON SOLUTIONS OF CUBIC NONLINEAR SCHRÖDINGER EQUATION WITH A MOMENTUM TERM", which he prepared after fulfilling the requirements specified in the associated legislations, before the jury whose signatures are below.

Thesis Advisor :	**Prof. Dr. İlkay BAKIRTAŞ AKAR** Istanbul Technical University	.....
Jury Members :	**Prof. Dr. Nalan ANTAR** Istanbul Technical University	.....
	Assoc. Prof. Dr. Mahmut BAĞCI Marmara University	.....

Date of Submission : **10 December 2024**
Date of Defense : **26 December 2024**

To my beloved mother,

FOREWORD

First and foremost, as the child of a family educated at ITU, I would like to express my deep connection to my university. I extend my gratitude to Prof. Dr. İlkay Bakırtaş Akar for giving me the opportunity to work on this topic during my Master's journey. While this journey has presented its challenges, their input has shaped my academic and character growth.

I would like to extend my heartfelt thanks to Res. Asst. Melis Turgut, who first entered my life as a teammate, later became my coworker, and ultimately my academic sister. Her unwavering support and protective presence have always been a source of reassurance throughout this process. Similarly, I want to thank my coworker Res. Asst. Şeyma Gönül, whose resilient character has been a huge inspiration. Starting this journey together as colleagues, we have always upheld a sense of solidarity, which has made this experience all the more meaningful.

I am deeply grateful to my strong friend Hazal Yürük for standing by my side, enduring my quirks, and supporting me through challenging times. She has been a great companion for my Master's journey, and our mutual resilience has been a constant source of strength.

Lastly, I would like to thank my family, each of whom has uniquely supported me throughout this endeavor. Their unwavering belief in me and the value they have placed on my success mean the world to me. A special note of gratitude goes to my mother, Gülcan, who has always been by my side and is the reason I am here today. Her unconditional love, dedication, and strength have been my greatest blessings.

This thesis is dedicated to my mother, Gülcan, the brilliant woman who gifted me my intellect and has always been my guiding light.

December 2024

Haldun Taha UZUNOĞLU
(Research Assistant)

TABLE OF CONTENTS

Page

FOREWORD ... **ix**
TABLE OF CONTENTS ... **xi**
ABBREVIATIONS ... **xiii**
LIST OF FIGURES ... **xv**
SUMMARY ... **xix**
ÖZET ... **xxi**
1. INTRODUCTION ... **1**
1.1 Purpose of Thesis ... 3
1.2 Literature Review ... 3
1.3 Hypothesis ... 5
2. NUMERICAL METHODS ... **7**
2.1 Spectral Renormalization Method ... 7
3. EFFECTS OF THE MOMEMTUM TERM AND PROPAGATION CONSTANT WITHOUT A $\mathscr{PT}$-SYMMETRIC POTENTIAL ... **11**
4. EXACT SOLUTIONS OF NLS EQUATION WITH A MOMENTUM TERM AND A $\mathscr{PT}$-SYMMETRIC POTENTIAL ... **15**
5. STABILITY ANALYSIS ... **23**
5.1 Split-Step Fourier Method ... 23
5.2 Nonlinear Stability Analysis ... 23
5.3 Linear Stability ... 36
5.3.1 Linear spectrum ... 36
6. CONCLUSION AND RECOMMENDATIONS ... **47**
REFERENCES ... **49**
APPENDIX A.1 ... 55
CURRICULUM VITAE ... **58**

ABBREVIATIONS

NLS	**:** Nonlinear Schrödinger
CNLS	**:** Cubic Nonlinear Schrödinger
3OD	**:** Third Order Dispersion
ODE	**:** Ordinary Differential Equation
$\mathscr{PT}$	**:** Parity - Time
SR	**:** Spectral Renormalization
Eq.	**:** Equation
Fig.	**:** Figure

LIST OF FIGURES

Page

Figure 3.1 : Existence region for varying values of Γ without an external potential..... 11

Figure 3.2 : Maximum amplitudes versus μ values for (a) $\Gamma = 0.1$, (b) $\Gamma = 1$ 12

Figure 3.3 : Stationary solitons of varying μ values for $\Gamma = 0.1$ and no external potential..... 12

Figure 3.4 : Stationary solitons of varying Γ values for $\mu = 1$ and no external potential..... 13

Figure 4.1 : The exact and numerical solutions of the NLS equation for $\mu = 1, W_1 = 1.5, V_2 = 1$ when (a) $\Gamma = 0$, (b) $\Gamma = 0.3$..... 19

Figure 4.2 : The exact and numerical solutions of the NLS equation for $\mu = 1, W_1 = 1, V_2 = 1.5$ when (a) $\Gamma = 0$, (b) $\Gamma = 0.3$..... 19

Figure 4.3 : The exact and numerical solutions of the NLS equation for $\mu = 1, W_1 = 0.5, V_2 = 1.5$ when (a) $\Gamma = -0.1$, (b) $\Gamma = -0.2$ 20

Figure 4.4 : Existence region of the NLS equation with $\mathscr{P}\mathscr{T}$-symmetric potential and momentum term for varying potential depths with $\mu = 1$ and (a) $\Gamma = 0$, (b) $\Gamma = 0.1$, (c) $\Gamma = 0.2$, (d) $\Gamma = 0.3$ 21

Figure 5.1 : Nonlinear stability of soliton for $\mu = 1$ and $\Gamma = 0$ without an external potential; (a) Numerically produced soliton (blue dashes) and the soliton after the evolution (purple solid), (b) Nonlinear evolution of the soliton, (c) The view from the top and (d) Maximum amplitude as a function of the propagation distance z. 24

Figure 5.2 : Nonlinear stability for $\mu = 1$ and $\Gamma = 1$ without an external potential; (a) Numerically produced soliton (blue dashes) and the soliton after the evolution (purple solid), (b) Nonlinear evolution of the soliton, (c) The view from the top and (d) Maximum amplitude as a function of the propagation distance z. 25

Figure 5.3 : Nonlinear stability for $\mu = 1$ and $\Gamma = 1.8$ without an external potential; (a) Numerically produced soliton (blue dashes) and the soliton after the evolution (purple solid), (b) Nonlinear evolution of the soliton, (c) The view from the top and (d) Maximum amplitude as a function of the propagation distance z. 25

Figure 5.4 : Nonlinear stability for $\mu = 1$ and $\Gamma = -1$ without an external potential; (a) Numerically produced soliton (blue dashes) and the soliton after the evolution (purple solid), (b) Nonlinear evolution of the soliton, (c) The view from the top and (d) Maximum amplitude as a function of the propagation distance z. 26

Figure 5.5 : Nonlinear stability for μ = 1 and $\Gamma = -1.8$ without an external potential; (a) Numerically produced soliton (blue dashes) and the soliton after the evolution (purple solid), (b) Nonlinear evolution of the soliton, (c) The view from the top and (d) Maximum amplitude as a function of the propagation distance z. 27

Figure 5.6 : Nonlinear stability for μ = 1, $\Gamma = 0$ and $W_1 = 0.5, V_2 = 0.5$ with a $\mathscr{P}\mathscr{T}$-symmetric potential; (a) Numerically produced soliton (blue dashes) and the soliton after the evolution (purple solid), (b) Nonlinear evolution of the soliton, (c) The view from the top and (d) Maximum amplitude as a function of the propagation distance z. 28

Figure 5.7 : Nonlinear stability for μ = 1, $\Gamma = 0$ and $W_1 = 0.5, V_2 = 2$ with a $\mathscr{P}\mathscr{T}$-symmetric potential; (a) Numerically produced soliton (blue dashes) and the soliton after the evolution (purple solid), (b) Nonlinear evolution of the soliton, (c) The view from the top and (d) Maximum amplitude as a function of the propagation distance z. 28

Figure 5.8 : Nonlinear instability for μ = 1, $\Gamma = 0$ and $W_1 = 1.5, V_2 = 0.5$ with a $\mathscr{P}\mathscr{T}$-symmetric potential; (a) Numerically produced soliton (blue dashes) and the soliton after the evolution (purple solid), (b) Nonlinear evolution of the soliton, (c) The view from the top and (d) Maximum amplitude as a function of the propagation distance z. 29

Figure 5.9 : Nonlinear stability for μ = 1, $\Gamma = 0$ and $W_1 = 1.5, V_2 = 2$ with a $\mathscr{P}\mathscr{T}$-symmetric potential; (a) Numerically produced soliton (blue dashes) and the soliton after the evolution (purple solid), (b) Nonlinear evolution of the soliton, (c) The view from the top and (d) Maximum amplitude as a function of the propagation distance z. 30

Figure 5.10: Nonlinear instability for μ = 1, $\Gamma = 0.1$ and $W_1 = 0.5, V_2 = 0.5$ with a $\mathscr{P}\mathscr{T}$-symmetric potential; (a) Numerically produced soliton (blue dashes) and the soliton after the evolution (purple solid), (b) Nonlinear evolution of the soliton, (c) The view from the top and (d) Maximum amplitude as a function of the propagation distance z. 31

Figure 5.11: Nonlinear instability for μ = 1, $\Gamma = 0.1$ and $W_1 = 1.5, V_2 = 0.5$ with a $\mathscr{P}\mathscr{T}$-symmetric potential; (a) Numerically produced soliton (blue dashes) and the soliton after the evolution (purple solid), (b) Nonlinear evolution of the soliton, (c) The view from the top and (d) Maximum amplitude as a function of the propagation distance z. 31

Figure 5.12: Nonlinear stability for μ = 1, $\Gamma = 0.1$ and $W_1 = 0.5, V_2 = 1.5$ with a $\mathscr{P}\mathscr{T}$-symmetric potential; (a) Numerically produced soliton (blue dashes) and the soliton after the evolution (purple solid), (b) Nonlinear evolution of the soliton, (c) The view from the top and (d) Maximum amplitude as a function of the propagation distance z. 32

Figure 5.13: Nonlinear instability for $\mu = 1$, $\Gamma = 0.2$ and $W_1 = 0.5, V_2 = 1.5$ with a $\mathscr{P}\mathscr{T}$-symmetric potential; (a) Numerically produced soliton (blue dashes) and the soliton after the evolution (purple solid), (b) Nonlinear evolution of the soliton, (c) The view from the top and (d) Maximum amplitude as a function of the propagation distance z. 33
Figure 5.14: Nonlinear instability for $\mu = 1$, $\Gamma = 0.2$ and $W_1 = 1.5, V_2 = 1.5$ with a $\mathscr{P}\mathscr{T}$-symmetric potential; (a) Numerically produced soliton (blue dashes) and the soliton after the evolution (purple solid), (b) Nonlinear evolution of the soliton, (c) The view from the top and (d) Maximum amplitude as a function of the propagation distance z. 33
Figure 5.15: Nonlinear instability for $\mu = 1$, $\Gamma = 0.4$ and $W_1 = 0.5, V_2 = 1$ with a $\mathscr{P}\mathscr{T}$-symmetric potential; (a) Numerically produced soliton (blue dashes) and the soliton after the evolution (purple solid), (b) Nonlinear evolution of the soliton, (c) The view from the top and (d) Maximum amplitude as a function of the propagation distance z. 34
Figure 5.16: Nonlinear instability for $\mu = 1$, $\Gamma = -0.1$ and $W_1 = 0.5, V_2 = 1.5$ with a $\mathscr{P}\mathscr{T}$-symmetric potential; (a) Numerically produced soliton (blue dashes) and the soliton after the evolution (purple solid), (b) Nonlinear evolution of the soliton, (c) The view from the top and (d) Maximum amplitude as a function of the propagation distance z. 35
Figure 5.17: Nonlinear instability for $\mu = 1$, $\Gamma = -0.2$ and $W_1 = 0.5, V_2 = 1.5$ with a $\mathscr{P}\mathscr{T}$-symmetric potential; (a) Numerically produced soliton (blue dashes) and the soliton after the evolution (purple solid), (b) Nonlinear evolution of the soliton, (c) The view from the top and (d) Maximum amplitude as a function of the propagation distance z. 35
Figure 5.18: Linear spectra of NLS equation for $\mu = 1$ without an external potential; (a) $\Gamma = 0$, (b) $\Gamma = 1$ 39
Figure 5.19: Linear spectra of NLS equation for $\mu = 1$ without an external potential; (a) $\Gamma = -1.8$, (b) $\Gamma = -1$ 40
Figure 5.20: Linear spectra of NLS equation for $\mu = 1$, $\Gamma = 0$ with a $\mathscr{P}\mathscr{T}$-symmetric potential; (a) $W_1 = 0.5, V_2 = 0.5$, (b) $W_1 = 0.5, V_2 = 2$ 41
Figure 5.21: Linear spectra of NLS equation for $\mu = 1$, $\Gamma = 0$ with a $\mathscr{P}\mathscr{T}$-symmetric potential; (a) $W_1 = 1.5, V_2 = 0.5$, (b) $W_1 = 1.5, V_2 = 2$ 42
Figure 5.22: Linear spectra of NLS equation for $\mu = 1$, $\Gamma = 0.1$ with a $\mathscr{P}\mathscr{T}$-symmetric potential; (a) $W_1 = 0.5, V_2 = 0.5$, (b) $W_1 = 1.5, V_2 = 0.5$ 43
Figure 5.23: Linear spectra of NLS equation for $\mu = 1, W_1 = 0.5, V_2 = 1.5$ with a $\mathscr{P}\mathscr{T}$-symmetric potential; (a) $\Gamma = 0.1$, (b) $\Gamma = 0.2$ 44
Figure 5.24: Linear spectra of NLS equation for $\mu = 1$ with a $\mathscr{P}\mathscr{T}$-symmetric potential; (a) $\Gamma = 0.2$, $W_1 = 1.5, V_2 = 1.5$, (b) $\Gamma = 0.4$ $W_1 = 0.5, V_2 = 1$ 45

Figure 5.25: Linear spectra of NLS equation for $\mu = 1$ with a $\mathscr{P}\mathscr{T}$-symmetric potential; (a) $\Gamma = -0.1$, $W_1 = 0.5, V_2 = 1.5$, (b) $\Gamma = -0.2$ $W_1 = 0.5, V_2 = 1.5$ 45

EXACT SOLITON SOLUTIONS OF CUBIC NONLINEAR SCHRÖDINGER EQUATION WITH A MOMENTUM TERM

SUMMARY

There are various interconnections between the positive sciences, with differential equations serving as a fundamental bridge linking mathematics to other scientific disciplines. Nonlinear wave phenomena have recently gained considerable attention due to their theoretical significance and applied relevance. Nonlinear optical wave equations not only facilitate the development of advanced techniques but also play a crucial role in elucidating natural phenomena across diverse fields, including biology, nonlinear optics, and quantum physics. Among these, solitons—localized nonlinear waves—stand out as valuable tools for understanding complex nonlinear systems. Solitons are widely studied in areas such as plasma physics, nonlinear optics, and quantum mechanics.

Optical solitons, in particular, have drawn significant interest due to the inherently interdisciplinary nature of soliton theory, making it a pivotal topic for advancing technologies like high-speed data transmission. The external potential strongly influences the shape and stability of optical pulses. In quantum mechanics and nonlinear optics, potentials with parity-time symmetry ($\mathscr{P}\mathscr{T}$-symmetry) are frequently utilized. Numerous studies in the literature examine the stability of nonlinear Schrödinger (NLS) equations with $\mathscr{P}\mathscr{T}$-symmetry. These equations admit various nonlinear wave solutions, including solitons, which are localized waves that propagate without distortion. Solitons demonstrate remarkable resilience during collisions, retaining their properties even after interacting with other waves.

This work investigates the soliton solutions and their stability in the NLS equation incorporating a momentum term and cubic nonlinearity under an external $\mathscr{P}\mathscr{T}$-symmetric potential. The governing equation is expressed as:

$$iu_z + \alpha u_{xx} - i\Gamma u_x + \phi |u|^2 u + V_{PT} u = 0.$$

Here, z denotes the scaled propagation distance, u is the differentiable complex-valued slowly varying amplitude, u_{xx} represents diffraction, Γ is the momentum term taken as a constant, and V_{PT} denotes the external potential. The $\mathscr{P}\mathscr{T}$-symmetric potential is defined as:

$$\begin{aligned} V_{PT} &= V(x) + iW(x) \\ &= \left[V_0 + V_1 \mathrm{sech}(x) + V_2 \mathrm{sech}^2(x)\right] \\ &\quad + i\left[W_0 \mathrm{sech}(x)\tanh(x) + W_1 \tanh(x)\right]. \end{aligned}$$

Here, $V(x)$ and $W(x)$ represent the real and imaginary components of the potential, where $V(x)$ is an even function and $W(x)$ is an odd function.

A detailed introduction to solitons and their interdisciplinary significance is provided in Chapter 1. The NLS equation is introduced, along with its recent developments,

including the momentum term and $\mathscr{P}\mathscr{T}$-symmetry. The chapter also outlines the research objectives and the thesis hypothesis, emphasizing the importance of the momentum term in the NLS equation.

Chapter 2 describes the Spectral Renormalization (SR) Method, an iterative Fourier technique used to numerically solve the NLS equation with a momentum term and a $\mathscr{P}\mathscr{T}$-symmetric potential. The method is adapted to the problem at hand, and numerical solutions are obtained.

In Chapter 3, the structure of the NLS equation without potential is analyzed to investigate the effect of the momentum term. Variations in soliton structures are examined in relation to changes in the momentum term coefficient, Γ, and the propagation constant, μ.

Chapter 4 explores exact solutions of the NLS equation with a momentum term and $\mathscr{P}\mathscr{T}$-symmetric potential. Using the ansatz $u(x,z) = f(x)e^{i(\mu z+g(x))}$, where $f(x)$ and $g(x)$ are real-valued functions, analytical solutions are derived. These solutions are compared with the numerical results, which shows excellent agreement. The chapter also verifies the parity-time symmetry properties of the potential, confirming that its imaginary part is odd and its real part is even.

Chapter 5 focuses on the stability analysis of soliton solutions. The Split-Step Fourier method is employed to investigate nonlinear stability, while linear stability is examined through the linear spectrum. The results indicate that the solitons become unstable with even slight increases in the momentum term coefficient, Γ. Additionally, enhancing the complex component of the potential increases instability, whereas increasing the real component improves stability.

The acquired results are summed up in Chapter 6. Moreover, a brief discussion on potential future research is included. All numerical results were obtained using MATLAB®.

MOMENTUM TERİMİ İÇEREN
KÜBİK NONLİNEER SCHRÖDINGER DENKLEMİNİN
SOLİTON TİPİ ÇÖZÜMLERİ

ÖZET

Pozitif bilimler arasında pek çok disiplinler arası ilişki bulunmaktadır ve diferansiyel denklemler, matematiğin diğer bilim dallarıyla etkileşimindeki kritik köprülerden birini oluşturur. Son yıllardaki çalışmalarda, doğrusal olmayan dalga problemleri hem teorik hem de uygulamalı bağlamlarda önemli bir ilgi odağı haline gelmiştir. Doğrusal olmayan optik dalga denklemleri, yalnızca yeni tekniklerin geliştirilmesine katkıda bulunmakla kalmaz, aynı zamanda biyoloji, doğrusal olmayan optik ve kuantum fiziği gibi birçok alanda doğanın temel mekanizmalarının anlaşılmasına da olanak sağlar. Bu bağlamda, lokalize doğrusal olmayan dalgalar olan solitonlar, karmaşık doğrusal olmayan sistemlerin çözümlenmesinde güçlü araçlar sunar. Solitonlar, plazma fiziği, doğrusal olmayan optik ve kuantum mekaniği gibi geniş bir bilimsel yelpazede karşımıza çıkar.

Optik solitonlar, disiplinler arası bir teori olan soliton teorisinin merkezinde yer aldıkları için özellikle dikkat çekmektedir. Soliton araştırmaları, özellikle veri aktarım teknolojilerinin geliştirilmesi açısından önem arz etmektedir. Kuantum mekaniği ve doğrusal olmayan optikte, parite-zaman simetrisine ($\mathscr{P}\mathscr{T}$-simetrisi) sahip potansiyeller yaygın olarak incelenmektedir. Literatürde, $\mathscr{P}\mathscr{T}$-simetrisi içeren doğrusal olmayan Schrödinger (NLS) denklemlerinin kararlılık analizine yönelik birçok çalışma bulunmaktadır. Bu tür denklemler, çeşitli doğrusal olmayan dalga biçimlerini tanımlar ve bu dalgalardan bazıları solitonlar olarak bilinir. Solitonlar, hızlarını ve şekillerini koruyarak ilerleyen lokalize dalgalar olup çarpışmalar sırasında özelliklerini kaybetmezler.

Literatürde, ikinci derece dispersiyon terimi ve kübik/kübik-kuintik doğrusal olmayanlık içeren NLS denkleminin analitik ve sayısal çözümleri kapsamlı bir şekilde ele alınmıştır. Bununla birlikte, ikinci derece dispersiyona ek olarak üçüncü derece dispersiyonun etkilerinin incelenmesi, kıtalar arası veri aktarımı gibi problemler için giderek daha fazla önem kazanmıştır. Optik atımların şekillerini ve kararlılıklarını etkileyen diğer bir kritik faktör ise dış optik potansiyellerdir. $\mathscr{P}\mathscr{T}$-simetrisi taşıyan potansiyeller, son yıllarda kuantum mekaniği problemlerinde yoğun bir şekilde araştırılmaktadır. Ancak, momentum terimi içeren NLS denklemleri literatürde daha yeni bir çalışma alanı olarak dikkat çekmektedir. Gross-Pitaevskii denklemi, dış potansiyel ve momentum terimi eklenmiş bir NLS denklemi olarak son yıllarda incelenmiştir.

Bu çalışmada, $\mathscr{P}\mathscr{T}$-simetrisine sahip bir dış potansiyelde momentum terimli ve kübik doğrusal olmayan bir NLS denkleminin soliton çözümleri ve kararlılık analizleri incelenmektedir. İncelenecek model aşağıdaki gibidir:

$$iu_z + \alpha u_{xx} - i\Gamma u_x + \phi|u|^2 u + V_{PT} u = 0.$$

Burada z ölçekli yayılma mesafesini, u türevlenebilir, karmaşık değerli, yavaşça artan genliği, u_{xx} kırınımı, Γ sabit bir momentum terimini ve V_{PT} dış potansiyeli temsil eder. Bu çalışmada ele alınan dış potansiyel şu şekilde tanımlanmıştır:

$$V_{PT} = V(x) + iW(x).$$

Burada $V(x)$ çift fonksiyon olarak gerçel kısmı, $W(x)$ ise tek fonksiyon olarak sanal kısmı ifade etmektedir.

Bölüm 1'de, soliton kavramı ve bu kavramın diğer bilimsel disiplinlerle ilişkisi ele alınmıştır. NLS denklemi tanıtılarak, bu denklemin momentum terimi ve $\mathscr{P}\mathscr{T}$-simetrisi ile genişletilmiş formu sunulmuştur. Literatür taramasının amacı, hipotez ve tez çalışmasının genel hedefleri açıklanmıştır. Ayrıca NLS denklemindeki momentum teriminin etkisi detaylandırılmıştır.

Spektral Renormalizasyon (SR) Yöntemi ile $\mathscr{P}\mathscr{T}$-simetrik potansiyel ve momentum terimli NLS denkleminin sayısal çözümleri Bölüm 2'de sunulmuştur. SR Yöntemi, iteratif bir Fourier tekniği olup bu çalışmada kullanılan NLS denklemine uyarlanmıştır. Sayısal çözümler, aşağıdaki başlangıç koşulu ile elde edilmiştir:

$$w_0 = e^{-x^2}.$$

Yakınsama kriteri, $|w_n - w_{n-1}| < 10^{-12}$ olarak belirlenmiştir. Ayrıca, elde edilen sayısal çözümler, $\mathscr{P}\mathscr{T}$-simetrik potansiyel ve momentum terimli NLS denklemini 10^{-10}'dan daha küçük bir mutlak hata ile sağlamaktadır.

Bölüm 3'te momentum teriminin etkisini incelemek amacıyla potansiyel içermeyen NLS denkleminin yapısı analiz edilmiştir. Momentum terimi katsayısı Γ'daki değişikliklerin ve μ yayılma sabitinin farklı değerlerinin soliton yapıları üzerindeki etkisi araştırılmıştır.

NLS denkleminin momentum terimi ve $\mathscr{P}\mathscr{T}$-simetrik potansiyele sahip kesin çözümleri Bölüm 4'te detaylı bir şekilde incelenmiştir. Bu bölümde, $\mathscr{P}\mathscr{T}$-simetrik potansiyelin yapısı oluşturulmuş ve analitik çözümler türetilmiştir. Önerilen çözüm,

$$u(x,z) = f(x)e^{i(\mu z + g(x))},$$

şeklinde ifade edilmekte olup, burada $f(x)$ ve $g(x)$ iki gerçek değerli fonksiyon olarak tanımlanmıştır. Bu çözüm, $\mathscr{P}\mathscr{T}$-simetrik potansiyelin kesin biçiminin belirlenmesine olanak tanımaktadır. Potansiyelin reel ve sanal kısımları sırasıyla şu şekilde elde edilmiştir:

$$V(x) = V_0 + V_1\mathrm{sech}(x) + V_2\mathrm{sech}^2(x),$$
$$W(x) = W_0\mathrm{sech}(x)\tanh(x) + W_1\tanh(x).$$

Burada $V(x)$ bir çift fonksiyon, $W(x)$ ise bir tek fonksiyon olarak $\mathscr{P}\mathscr{T}$-simetrik yapıdaki potansiyeli tanımlamaktadır. Elde edilen toplam potansiyel şu şekilde ifade edilmiştir:

$$\begin{aligned} V_{PT} = &\left[V_0 + V_1\mathrm{sech}(x) + V_2\mathrm{sech}^2(x)\right] \\ &+ i\left[W_0\mathrm{sech}(x)\tanh(x) + W_1\tanh(x)\right]. \end{aligned}$$

Sayısal çözümler ile analitik çözümler karşılaştırılmış ve bu çözümler üst üste çizilerek görselleştirilmiştir. İlgili grafikler, SR yönteminin bu tür denklemler için uygun

bir çözüm yöntemi olduğunu açıkça göstermektedir. Analitik ve sayısal çözümler arasındaki güçlü uyum, yöntemin doğruluğunu ve etkinliğini doğrulamaktadır.

Momentum terimi ve $\mathscr{P}\mathscr{T}$-simetrik potansiyele sahip NLS denkleminin kararlılık analizi Bölüm 5'te ele alınmıştır. Bu bölümde, elde edilen solitonların kararlılığı, ayrık adımlı Fourier metodu kullanılarak analiz edilmiştir. Bu yöntem, doğrusal olmayan stabilite özelliklerini değerlendirmede etkili bir yaklaşımdır. Ek olarak, lineer stabilite analizi yapılmış ve bu amaçla lineer spektrum analizinden yararlanılmıştır. Çeşitli Γ değerleri için lineer spektrumlar incelenmiş ve momentum terimi katsayısı Γ'daki küçük bir artışın dahi solitonları kararsız hale getirdiği gözlemlenmiştir. Ayrıca potansiyelin sanal kısmındaki artış, solitonların kararsızlığını artırırken, reel kısmındaki artış daha kararlı yapılar ortaya çıkarmaktadır.

Elde edilen sonuçlar, Bölüm 6'da özetlenmiştir. Ayrıca, gelecekte yapılabilecek olası araştırmalar hakkında kısa bir tartışmaya yer verilmiştir. Tüm sayısal analizler ve grafikler, MATLAB® yazılımı kullanılarak elde edilmiştir.

1. INTRODUCTION

Numerous domains, including quantum mechanics, nonlinear optics, and biology, have conducted extensive theoretical and experimental research on solitary waves, also known as solitons [1]. It is well known that a soliton is a solitary wave that, in the event of nonlinear interaction with other solitary waves, asymptotically maintains its shape and velocity [2]. Any optical field that remains unchanged during transmission as a result of the medium's balance between linear and nonlinear effects is referred to as a soliton in optics [3]. Since solitons provide advantages for understanding complex situations, they can be utilized to expedite complex experiments. Solitons are categorized as temporal or spatial in the setting of nonlinear optics based on whether light confinement happens in time or space during wave propagation. While spatial solitons are self-guided beams that stay limited in the transfer directions orthogonal to the direction of propagation, temporal solitons are optical pulses that hold their shape. A pulse or beam is said to be self-localized when it travels through a medium without changing shape in either scenario [3]. One significant nonlinear evolution equation that utilized in various fields of applied mathematics and physics is the nonlinear Schrödinger (NLS) equation. The NLS equation is named after its resemblance to the well-known Schrödinger equation derived by Erwin Schrödinger, which is central to quantum mechanics and describes the wave function of a particle in a potential. [4]. However, while the Schrödinger equation is a fundamental aspect of quantum theory, the NLS arises from classical wave theory, particularly in the context of nonlinear optics and fluid dynamics. The NLS describes the evolution of wave packets in nonlinear, dispersive environments, where the nonlinearity can significantly affect wave propagation. NLS equation was first solved in 1971 using the inverse scattering theory by Zakharov and Shabat. In their groundbreaking work, they provided a method to study the propagation of pulses in nonlinear waveguides, incorporating both nonlinearity and dispersion [5].

NLS equation is given as follows, with pulses at a time scale of 1 picosecond:

$$iu_z + u_{xx} + \alpha|u|^2 u = 0. \tag{1.1}$$

where u is the differentiable complex-valued, progressively changing amplitude of the electric field, u_{xx} denotes diffraction and z is a scaled propagation distance. The coefficient α indicates the sign of the medium's cubic nonlinearity. This NLS equation is the simplest form of the NLS equation and is known as being (1+1)-dimensional. The selection of α results in $+1$ and -1 for the bright and dark spatial solitons, respectively. Only the bright soliton type of solution is taken into consideration in this thesis.

The cubic nonlinear Schrödinger equation with $\mathscr{P}\mathscr{T}$-symmetric optical potential and momentum term given below is investigated:

$$iu_z + \alpha u_{xx} - i\Gamma u_x + \phi|u|^2 u + V_{PT} u = 0. \tag{1.2}$$

Here, Γ is the coefficient of the momentum term which can be taken as a positive or a negative value and V_{PT} is a $\mathscr{P}\mathscr{T}$-symmetric external potential which the exact structure is defined in Chapter 3. The coefficient of the cubic term ϕ will be taken as $\phi = 1$ in this thesis.

The $\mathscr{P}\mathscr{T}$-symmetric potential will be considered as:

$$V_{PT} = V(x) + iW(x) \tag{1.3}$$

This thesis aims to investigate the exact and numerical solutions of equation (1.2) and ascertain the impact of the momentum term $i\Gamma u_x$ on the stabilities of the soliton solutions.

The Spectral Renormalization (SR) method is used to solve Eq. (1.2). This approach, fundamentally a Fourier-based iterative technique, was initially proposed by Petviashvili in 1975 [6]. The method was first employed to identify localized solutions for the two-dimensional Korteweg-deVries equation, commonly known as the Kadomtsev-Petviashvili (KP) equation [7]. Subsequently, Ablowitz and Musslimani refined the method in the early 2000s [8]. The SR method works by converting the governing soliton equation—such as an NLS-type equation—into Fourier space, leading to a nonlocal integral equation coupled with an algebraic equation. This

coupling mechanism ensures numerical stability and prevents divergence during iterations.

1.1 Purpose of Thesis

In this thesis, how the soliton solutions of the cubic nonlinear Schrödinger equation with $\mathscr{PT}$-symmetric potential and momentum term are affected by the external potential and momentum term is studied. It is aimed to find exact and numerical soliton type solutions of this model and investigate the linear and nonlinear stability characteristics of the obtained solitons.

1.2 Literature Review

Many mathematical and physical disciplines, including nonlinear optics, plasma physics, and quantum mechanics, deal with nonlinear wave problems [9–11]. Scientists have been debating the solutions and stabilities of the NLS equations for a long time [2, 3, 12, 13]. Solitons can be found as the solutions to a common class of ordinary differential equations that describe physical systems and are weakly nonlinear and dispersive [14]. Kartashov, Vysloukh, and Torner's recent work discusses lattice solitons, which are relevant to various types of optical lattices and their potential stabilization [15]. Musslimani and colleagues investigate the stability of optical solitons in a periodic $\mathscr{PT}$-symmetric potential [16]. Numerous scientists investigate optical soliton solutions of NLS equations using $\mathscr{PT}$-symmetric optical lattices [17–20]. It was discovered that in parity-time symmetric mixed linear-nonlinear optical lattices, lattice solitons exist and are stable. Additionally, it is shown that the linear lattice periodic potential's parameters play a significant role in regulating stability domain areas [21]. The existence and stability characteristics of solitons of the (1+1)D cubic-quintic NLS equations with $\mathscr{PT}$-symmetric external potential were studied by Göksel et al [22]. They employed the SR method to derive solutions for various potential depths and explored the soliton stability and instability regions using linear spectrum analysis.

In saturable media, the numerical existence of fundamental solitons in crystal and certain quasicrystal lattices was studied. Their nonlinear stability was assessed through numerical methods like the finite difference method and the fourth-order Runge-Kutta

method, while the influence of potential depth and applied external electrical fields on gap widths was also examined [23, 24]. Furthermore, soliton existence and stability in $\mathscr{PT}$-symmetric optical lattices with spatial modulation of nonlinearity were analyzed, revealing how these modulations affect stability [25].

Karlsson focused on the impact of higher-order dispersion in cubic NLS equations, specifically examining fourth-order dispersive terms without considering third-order dispersion [26]. Wazwaz and Kaur explored exact analytical solutions to NLS equations with normal dispersion using the variational iteration method. Additionally, soliton solutions for cubic NLS equations were generated, and canonical transformations were applied to solve NLS equations with cubic and quintic nonlinearities under time-dependent, inhomogeneous external potentials [27]. Soliton type solutions of cubic NLS equations are produced [28, 29]. The exact solutions of the nonlinear Schrödinger equation (NLS) with cubic and quintic nonlinearity were obtained through canonical transformations, considering time-dependent and inhomogeneous external potentials. In these studies, the role of $\mathscr{PT}$-symmetry was emphasized to ensure the conservation of the system's average energy. Stability and band-gap structures of higher-order NLS equations in periodic lattices were also analyzed [30].

Recent research primarily focuses on the dynamics of solitons in higher-dimensional, multi-order NLS equations [31, 32]. Yan and Chen investigated the stability of bright solitons in generalized NLS equations with various $\mathscr{PT}$-symmetric potentials, validating their stability using the linear stability spectrum. They also studied interactions between two solitons [33].

In quantum mechanics, Hamiltonians are typically expected to be Hermitian to guarantee real eigenvalues. However, recent studies by Bender and collaborators have shown that this Hermiticity condition is not necessary for real spectra, provided the system possesses $\mathscr{PT}$-symmetry. This groundbreaking result has broadened the understanding of quantum systems and their mathematical foundations [34, 35].

The effects of momentum term with NLS equation of higher order is investigated by Abdou and his colleagues using Scarf II potential [36]. Using the $\mathscr{PT}$-symmetric potential, Yan investigated both the stable solitons of the NLS equation and the

generalized Gross-Pitaevskii equation [37, 38]. In the literature, studies on exact analytical and numerical solutions of extended NLS equations with $\mathscr{PT}$-symmetric potential with a momentum term are still in their infancy. Due to the scarcity of research in this area, it has been deemed a suitable topic for investigation in this thesis.

1.3 Hypothesis

An extra momentum term has a significant effect on the existence and stability characteristics of the solutions to the cubic NLS equation with a $\mathscr{PT}$-symmetric potential. Furthermore, the linear and the nonlinear stability properties of the generated solitons are also analyzed and significant changes are observed by the inclusion of momentum effect. An additional momentum term causes Eq. (1.2) to be more unstable, and the potential depths of the $\mathscr{PT}$-symmetric potential also affect the presence and stability of the soliton type solutions of Eq. (1.2).

2. NUMERICAL METHODS

In this chapter, to determine the numerical solution to Eq. (1.2), the well-known Spectral Renormalization (SR) Method will be modified.

2.1 Spectral Renormalization Method

Numerous numerical techniques are available for obtaining solutions to NLS type equations. One of these methods, the SR method, is essentially Petviashvili's Fourier iteration used to find localized solutions for the two-dimensional Korteweg-deVries (KdV) equation. Afterwards, Ablowitz and Musslimani expanded on this technique by computing self-localized states using nonlinear wave guides [2]. This technique can be applied to numerous nonlinear systems involving nonlinearities with diverse homogeneities, such as cubic-quintic or as saturable nonlinearity, and it can be used to compute the self-localized states of nonlinear wave guides.

The cubic NLS equation with a $\mathscr{P}\mathscr{T}$-symmetric potential and momentum term can be solved using this method in the following way

$$iu_z + u_{xx} - i\Gamma u_x + |u|^2 u + V_{PT} u = 0. \tag{2.1}$$

by setting $\alpha = 1$ in Eq. (1.2). Using the ansatz $u(x,z) = f(x)e^{i\mu z}$ where $f(x)$ is a complex-valued function and μ is the propagation constant, one obtains:

$$\begin{aligned} u_z &= i\mu f e^{i\mu z} \\ u_x &= f_x e^{i\mu z} \\ u_{xx} &= f_{xx} e^{i\mu z} \\ |u|^2 &= |f|^2. \end{aligned} \tag{2.2}$$

The following nonlinear equation for f can be found by substituting the equations Eq. (2.2) into Eq. (2.1)

$$-\mu f e^{i\mu z} + f_{xx} e^{i\mu z} - i\Gamma f_x e^{i\mu z} + |f|^2 f e^{i\mu z} + V_{PT} f e^{i\mu z} = 0. \tag{2.3}$$

Upon eliminating the exponential term, the equation becomes

$$-\mu f + f_{xx} + i\Gamma f_x + |f|^2 f + V_{PT} f = 0. \tag{2.4}$$

By using the Fourier transform on Equation (2.4), one obtains

$$\mathscr{F}\{-\mu f\} + \mathscr{F}\{f_{xx}\} - \mathscr{F}\{i\Gamma f_x\} + \mathscr{F}\{|f|^2 f\} + \mathscr{F}\{V_{PT} f\} = \mathscr{F}\{0\}. \tag{2.5}$$

where $\mathscr{F}$ indicates Fourier transformation. Due to the properties of this transformation, one gets Eq. (2.6) as

$$-\mu \hat{f} - (k_x)^2 \hat{f} + \Gamma k_x \hat{f} + \mathscr{F}\{|f|^2 f\} + \mathscr{F}\{V_{PT} f\} = 0. \tag{2.6}$$

where $\mathscr{F}(f) = \hat{f}$ and k_x being Fourier variable. Solving Eq. (2.6) for $\hat{f}$ yields

$$\hat{f} = \frac{\mathscr{F}\{|f|^2 f\} + \mathscr{F}\{(V_{PT}) f\}}{\mu + (k_x)^2 - \Gamma k_x}. \tag{2.7}$$

It is not possible to find $f(x)$ using equation (2.7) since the scheme diverges. It is possible to determine the new field variable $f(x) = \lambda w(x)$, where λ is a parameter and $\lambda \in \mathbb{R}^+$. Once the new field variable $f(x)$ is arranged in equation (2.7), one obtains

$$\lambda \hat{w} = \frac{\mathscr{F}\{|w|^2 |\lambda|^2 \lambda w\} + \mathscr{F}\{(V_{PT}) \lambda w\}}{\mu + k_x^2 - \Gamma k_x}. \tag{2.8}$$

By simplifying the equation, $\hat{w}$ is found as

$$\hat{w} = \frac{\mathscr{F}\{|w|^2 |\lambda|^2 w\} + \mathscr{F}\{(V_{PT}) w\}}{\mu + k_x^2 - \Gamma k_x}. \tag{2.9}$$

To find out w, one can use Eq. (2.9) in an iterative manner. Additionally, to investigate $\hat{w}$, one can use the subsequent iteration approach:

$$\hat{w}_{n+1} = \frac{|\lambda|^2 \mathscr{F}\{|w_n|^2 w_n\} + \mathscr{F}\{V_{PT} w_n\}}{\mu + k_x^2 - \Gamma k_x}, \quad n \in \mathbb{N}. \tag{2.10}$$

with a Gaussian-type function chosen as the initial condition

$$w_0 = e^{-x^2}, \tag{2.11}$$

where $|w_{n+1} - w_n| < 10^{-12}$ is the convergence criterion. After multiplying both sides of Eq. (2.9) by $(\mu + k_x^2 - \Gamma k_x)$, one gets

$$(\mu + k_x^2 - \Gamma k_x)\hat{w} = |\lambda|^2 \mathscr{F}\{|w|^2 w\} + \mathscr{F}\{V_{PT} w\}. \tag{2.12}$$

By taking all terms of Eq. (2.12) to one side, the equation becomes

$$(\mu + k_x^2 - \Gamma k_x)\hat{w} - |\lambda|^2 \mathscr{F}\{|w|^2 w\} - \mathscr{F}\{V_{PT} w\} = 0. \tag{2.13}$$

After multiplying Eq. (2.13) by the conjugate of $\hat{w}$, i.e. by $\hat{w}^*$, one obtains

$$(\mu + k_x^2 - \Gamma k_x)|w|^2 - |\lambda|^2 \mathscr{F}\{|w|^2 w\}\hat{w}^* - \mathscr{F}\{V_{PT} w\}\hat{w}^* = 0. \tag{2.14}$$

Integrating Eq. (2.14) gives

$$\begin{aligned} -\int_{-\infty}^{\infty} (\mu + k_x^2 - \Gamma k_x)|w|^2 dk + |\lambda|^2 \int_{-\infty}^{\infty} \mathscr{F}\{|w|^2 w\}\hat{w}^* dk \\ + \int_{-\infty}^{\infty} \mathscr{F}\{V_{PT} w\}\hat{w}^* dk = 0. \end{aligned} \tag{2.15}$$

or in a more compact form

$$\begin{aligned} -\int_{-\infty}^{\infty} [(\mu + k_x^2 - \Gamma k_x)|w|^2 - \mathscr{F}\{V_{PT} w\}\hat{w}^*] dk \\ + |\lambda|^2 \int_{-\infty}^{\infty} \mathscr{F}\{|w|^2 w\}\hat{w}^* dk = 0. \end{aligned} \tag{2.16}$$

From Eq. (2.16), λ can be precisely computed as

$$|\lambda|^2 = \frac{\int_{-\infty}^{\infty} [(\mu + k_x^2 - \Gamma k_x)|w|^2 - \mathscr{F}\{V_{PT} w\}\hat{w}^*] dk}{\int_{-\infty}^{\infty} \mathscr{F}\{|w|^2 w\}\hat{w}^* dk}. \tag{2.17}$$

Thus, the eigenvalue λ can be calculated from Eq. (2.17). The proper soliton for the iteration's convergence is $f(x) = \lambda w(x) = \lambda \mathscr{F}^{-1}(\hat{w})$.

3. EFFECTS OF THE MOMEMTUM TERM AND PROPAGATION CONSTANT WITHOUT A $\mathscr{PT}$-SYMMETRIC POTENTIAL

In this chapter, the effect of the momentum term on soliton solutions of Eq. (2.1) without a $\mathscr{PT}$-symmetric potential will be examined.

For the numerical solution found in Chapter 2 using the ansatz $u(x,z) = f(x)e^{i\mu z}$ is shown in Fig. 3.1.

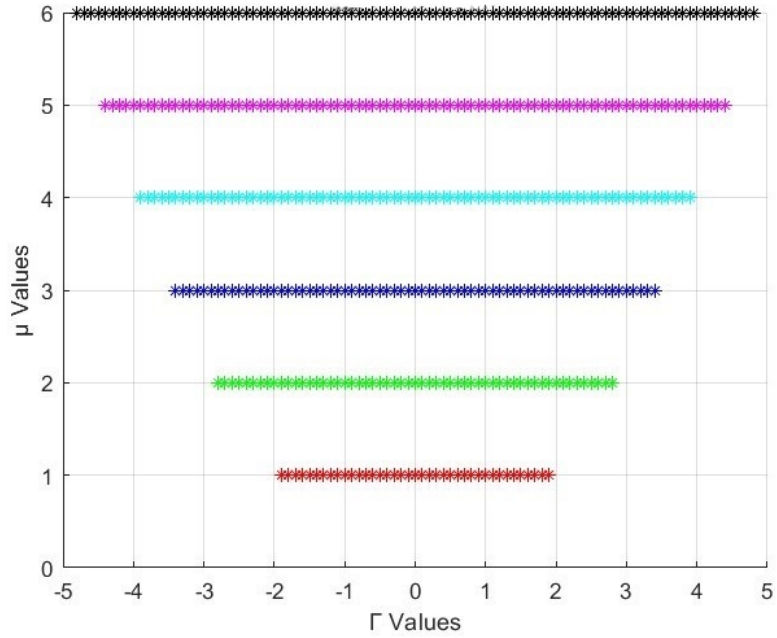

Figure 3.1 : Existence region for varying values of Γ without an external potential

The investigation is conducted for the values of $1 \leq \mu \leq 6$ to Eq. (2.1). When μ is equal to $\mu = 1$, the NLS equation has an existence range for $-1.9 \leq \Gamma \leq 1.9$. As μ increases, this existence range for Γ also expands. For instance, when μ reaches $\mu = 6$, the existence range of Γ extends for $-4.8 \leq \Gamma \leq 4.8$.

The propagation constant μ also has a significant impact on the amplitudes of solitons. In Fig. 3.2, the change in the amplitudes of the stationary states of solitons is shown for $1 \leq \mu \leq 10$.

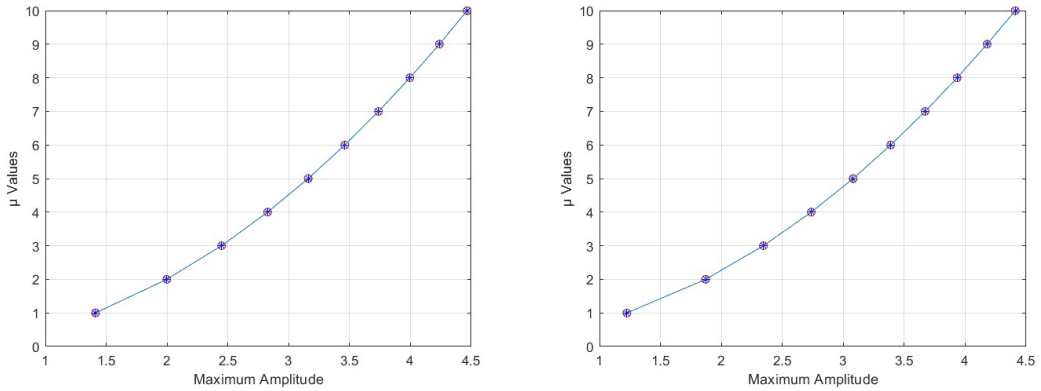

(a) **(b)**

Figure 3.2 : Maximum amplitudes versus μ values for (a) $\Gamma = 0.1$, (b) $\Gamma = 1$

It is observed that as μ increases, the amplitudes of the solitons progressively increase. When Γ is increased from $\Gamma = 0.1$ to $\Gamma = 1$, a slight decrease in the amplitudes can be observed.

To closely observe the changes in amplitudes, solitons calculated by SR method for different values of μ are plotted on top of each other, as shown in Fig. 3.3.

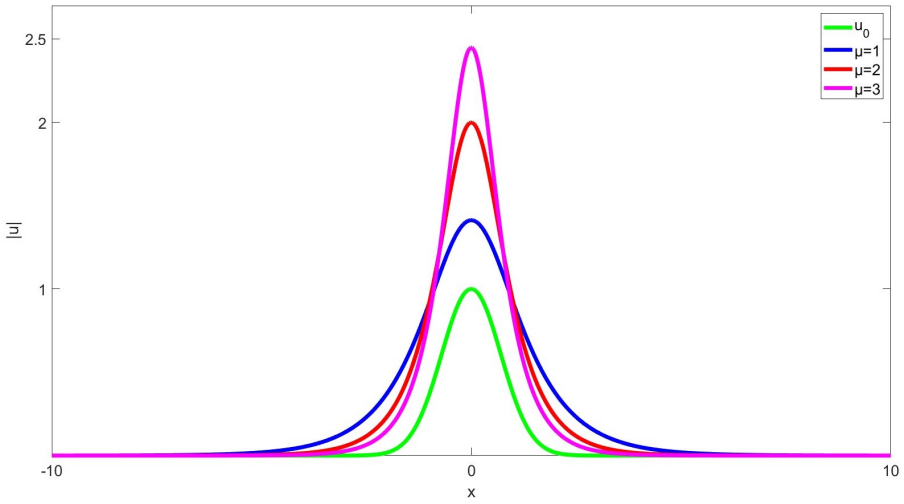

Figure 3.3 : Stationary solitons of varying μ values for $\Gamma = 0.1$ and no external potential.

Here, the case of $\Gamma = 0.1$ is examined, and with each increase in μ, the increment in the amplitude of the soliton is observed. A similar analysis can be performed by keeping μ fixed at $\mu = 1$ and plotting solitons for various values of Γ on top of each other.

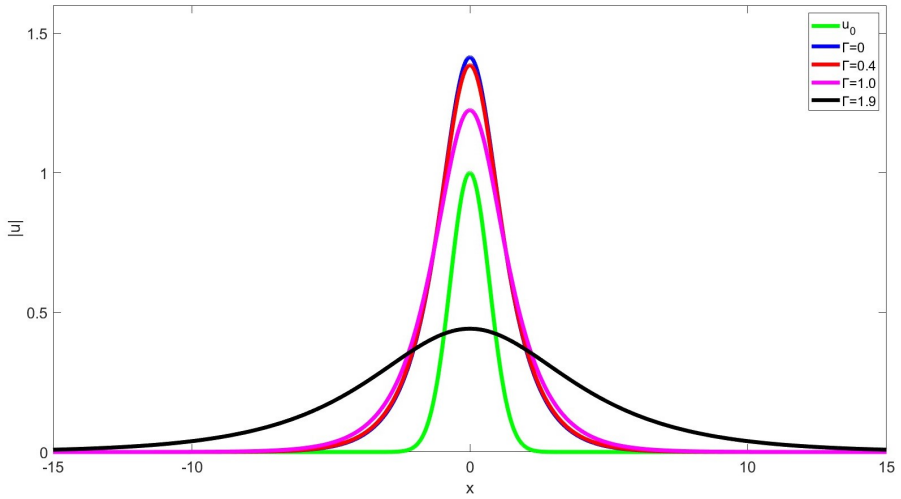

Figure 3.4 : Stationary solitons of varying Γ values for $\mu = 1$ and no external potential.

In Fig. 3.4, solitons are plotted for Γ values increasing namely for $\Gamma = 0, 0.4, 1, 1.9$. As can be seen from the figure, for a fixed μ, the increment in Γ values progressively decreases the amplitude of the solitons.

4. EXACT SOLUTIONS OF NLS EQUATION WITH A MOMENTUM TERM AND A $\mathscr{PT}$-SYMMETRIC POTENTIAL

The exact soliton type solution of the NLS equation with a $\mathscr{PT}$-symmetric external potential and momentum term will be obtained in this chapter. This equation is given as:

$$iu_z + \alpha u_{xx} - i\Gamma u_x + |u|^2 u + V_{PT} u = 0. \tag{4.1}$$

For $u = 0$, the trivial solution of Eq. (4.1) can be found. In order to find non-zero solutions, consider $u \neq 0$. Dividing Eq. (4.1) by u and considering $V_{PT} = V(x) + iW(x)$ gives

$$i\frac{u_z}{u} + \frac{\alpha u_{xx}}{u} - i\Gamma\frac{u_x}{u} + |u|^2 + V + iW = 0. \tag{4.2}$$

The following ansatz is used to find non-zero stationary solitons:

$$u(x,z) = f(x)e^{i(\mu z + g(x))}, \tag{4.3}$$

where $f(x)$ and $g(x)$ are real-valued nonzero functions that are distinct from zero, u is a function of x and z and to be determined, and μ is the propagation constant. By deriving u with respect to z and x, one obtains:

$$\begin{aligned}
u_z &= f(x)i\mu e^{i(\mu z+g(x))} = i\mu u,\\
u_x &= f'(x)e^{i(\mu z+g(x))} + ig'f(x)e^{i(\mu z+g(x))} = f'(x)\frac{u}{f} + ig'(x)u,\\
u_{xx} &= \left[f''(x) + 2if'(x)g'(x) + if(x)g''(x) - f(x)(g'(x))^2\right]e^{i(\mu z+g(x))}\\
&= \frac{u}{f}\left[f''(x) + 2if'(x)g'(x) + if(x)g''(x) - f(x)(g'(x))^2\right],\\
|u|^2 &= f(x)e^{i(\mu z+g(x))}f(x)e^{-i(\mu z+g(x))} = (f(x))^2.
\end{aligned} \tag{4.4}$$

Substituting Eq. (4.4) into Eq. (4.2) yields

$$\begin{aligned}
&[-\mu + \alpha\frac{f''(x)}{f(x)} - \alpha(g'(x))^2 + \Gamma g'(x) + |f|^2 + V(x)]\\
&+ i[2\alpha\frac{f'(x)g'(x)}{f(x)} + \alpha g''(x) - \Gamma\frac{f'(x)}{f(x)} + W(x)] = 0.
\end{aligned} \tag{4.5}$$

The following ansatzs are used for investigation of soliton solutions:

$$\begin{aligned} f(x) &= f_0 \text{sech}^p(x), \\ g'(x) &= g_0 \text{sech}^q(x), \end{aligned} \tag{4.6}$$

where f_0 and g_0 are non-zero real constants and $p, q \in \mathbb{N}$. By using Eq. (4.6) the necessary derivatives are obtained as

$$\begin{aligned} f'(x) &= -fp\tanh(x), \\ f''(x) &= f\left[p^2 - (p^2+p)\text{sech}^2(x),\right] \\ g'(x) &= g_0 \text{sech}^q(x), \\ g''(x) &= -g'q\tanh(x). \end{aligned} \tag{4.7}$$

By substituting Eq. (4.7) into Eq. (4.5), one gets

$$\begin{aligned} &[-\mu + \alpha p^2 - \alpha(p^2+p)\text{sech}^2(x) \\ &- ag_0^2\text{sech}^{2q}(x) + \Gamma g_0 \text{sech}^q(x) + f_0^2 \text{sech}^{2p}(x) + V(x)] \\ &+ i[-\alpha g_0(2p+q)\text{sech}^q(x)\tanh(x) + \Gamma p\tanh(x) + W(x)] = 0. \end{aligned} \tag{4.8}$$

To get real and imaginary parts of the $\mathscr{P}\mathscr{T}$-symmetric potential, Eq. (4.8) can be splitted into two parts as:

Real Part

The real part of Eq. (4.8) can be expressed as

$$\begin{aligned} -\mu + \alpha p^2 - \alpha(p^2+p)\text{sech}^2(x) - \alpha g_0^2 \text{sech}^{2q}(x) \\ \Gamma g_0 \text{sech}^q(x) + f_0^2 \text{sech}^{2p}(x) + V(x) = 0. \end{aligned} \tag{4.9}$$

The real part of the $\mathscr{P}\mathscr{T}$-symmetric potential is found as

$$\begin{aligned} V(x) = V_0 + V_1 \text{sech}^2(x) + V_2 \text{sech}^q(x) \\ + V_3 \text{sech}^{2q}(x) + V_4 \text{sech}^{2p}(x), \end{aligned} \tag{4.10}$$

where

$$\begin{aligned} V_0 &= \mu - \alpha p^2 \\ V_1 &= \alpha(p^2+p) \\ V_2 &= -\Gamma g_0 \\ V_3 &= \alpha g_0^2 \\ V_4 &= -f_0^2. \end{aligned} \tag{4.11}$$

It is seen in the following form that V(x) is an even function:

$$\begin{aligned} V(-x) &= V_0 + V_1\text{sech}^2(-x) + V_2\text{sech}^q(-x) \\ &\quad + V_3\text{sech}^{2q}(-x) + V_4\text{sech}^{2p}(-x) \\ &= V_0 + V_1\text{sech}^2(x) + V_2\text{sech}^q(x) \\ &\quad + V_3\text{sech}^{2q}(x) + V_4\text{sech}^{2p}(x) \\ &= V(x). \end{aligned} \tag{4.12}$$

$V(x)$ can be expressed by the powers of sech(x). For $p = q = 1$ Eq. (4.10) can be rewritten as:

$$\begin{aligned} V(x) &= \mu - \alpha + 2\alpha\text{sech}^2(x) - \Gamma g_0\text{sech}(x) \\ &\quad + \alpha g_0^2\text{sech}^2(x) - f_0^2\text{sech}^2(x). \end{aligned} \tag{4.13}$$

$V(x)$ is simplified as

$$V(x) = (\mu - \alpha) + (-\Gamma g_0)\text{sech}(x) + (2\alpha + \alpha g_0^2 - f_0^2)\text{sech}^2(x), \tag{4.14}$$

where

$$\begin{aligned} V_0 &= \mu - \alpha \\ V_1 &= -\Gamma g_0 \\ V_2 &= 2\alpha + \alpha g_0^2 - f_0^2. \end{aligned} \tag{4.15}$$

The real part of the $\mathscr{P}\mathscr{T}$-symmetric potential is obtained as

$$V(x) = \mu - \alpha - \Gamma g_0\text{sech}(x) + (2\alpha + \alpha g_0^2 - f_0^2)\text{sech}^2(x). \tag{4.16}$$

Imaginary Part

The complex part of Eq. (4.8) can be expressed as

$$\Gamma p\tanh(x) - \alpha g_0(2p+q)\text{sech}^q(x)\tanh(x) + W(x) = 0. \tag{4.17}$$

The imaginary part of the $\mathscr{P}\mathscr{T}$-symmetric potential is obtained as

$$W(x) = W_0\tanh(x) + W_1\text{sech}^q(x)\tanh(x), \tag{4.18}$$

where

$$\begin{aligned} W_0 &= -\Gamma p \\ W_1 &= \alpha g_0(2p+q). \end{aligned} \tag{4.19}$$

It can be seen that $W(x)$ is an odd function since:

$$\begin{aligned} W(-x) &= W_0 \tanh(-x) + W_1 \operatorname{sech}^q(-x)\tanh(-x) \\ &= -W_0 \tanh(x) - W_1 \operatorname{sech}^q(x)\tanh(-x) \\ &= -W(x). \end{aligned} \tag{4.20}$$

For $p = q = 1$, then Eq. (4.18) can be simplified to the following form,

$$W(x) = -\Gamma \tanh(x) + 3\alpha g_0 \operatorname{sech}(x)\tanh(x), \tag{4.21}$$

where

$$\begin{aligned} W_0 &= -\Gamma \\ W_1 &= 3\alpha g_0. \end{aligned} \tag{4.22}$$

The equations (4.15), (4.22) put a constraint on the potential depths: $V_2 < 2 + \frac{W_1^2}{9}$ for $\alpha = 1$. For the case of $p = q = 1$, the analytical solution of the problem can be suggested as

$$u(x,z) = f_0 \operatorname{sech}(x) e^{i[\mu z + g_0 \operatorname{arctanh}(x)\sinh(x)]}, \tag{4.23}$$

where $f_0 = \sqrt{2 + \frac{W_1^2}{9} - V_2}$ and $g_0 = \frac{W_1}{3}$. Hence, Eq. (1.2), with the real and the imaginary parts can be given as

$$V_{PT} = [V_0 + V_1 \operatorname{sech}(x) + V_2 \operatorname{sech}^2(x)] + i[W_0 \operatorname{sech}(x)\tanh(x) + W_1 \tanh(x)]. \tag{4.24}$$

For Kerr medium, Eq. (4.24) can be interpreted as an extension of the Scarf II potential [39].

In Fig. 4.1, the soliton produced analytically, as previously mentioned, is displayed with a dashed purple solid line, whereas the soliton obtained numerically using the SR method, as explained in Chapter 2, is plotted with a blue solid line. The image illustrates how two solitons overlap, and the numerical solution that was found satisfies Eq. (2.1) with an absolute error of 10^{-7}. As a result, it demonstrates that the SR approach is appropriate for solving this equation and that the analytical solution is proven to be correct.

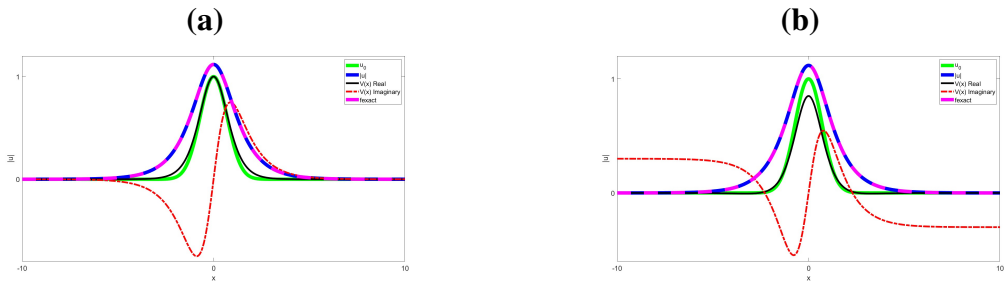

Figure 4.1 : The exact and numerical solutions of the NLS equation for $\mu = 1, W_1 = 1.5, V_2 = 1$ when (a) $\Gamma = 0$, (b) $\Gamma = 0.3$

In Fig. 4.1, the behavior of the potential is also depicted for when there is no effect of the momentum term and when $\Gamma = 0.3$. The black solid line represents the real part of the potential, while the red dashed line represents the imaginary part. The values of W_1 and V_2 for the calculated potential were manually chosen, with $W_1 = 1.5$ and $V_2 = 1$. It is observed that for different Γ values, the depths of the potential vary, indicating changes in the structure of the potential due to its dependence on Γ.

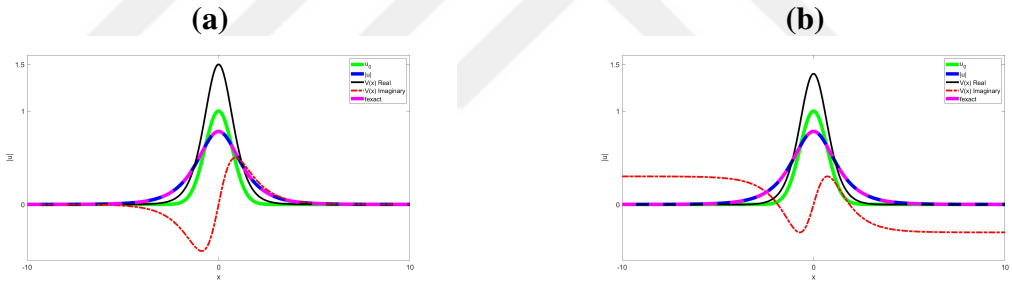

Figure 4.2 : The exact and numerical solutions of the NLS equation for $\mu = 1, W_1 = 1, V_2 = 1.5$ when (a) $\Gamma = 0$, (b) $\Gamma = 0.3$

In Fig. 4.2, the depth of the complex part of the potential, represented by W_1, has been reduced, while the depth of the real part, represented by V_2, has been increased. It can be seen that the amplitude of the real part of the potential has increased, while the maximum amplitude of the imaginary part has decreased. Similarly, Fig. 4.1 and Fig. 4.2 show that an increase in Γ decreases the amplitudes of both the real and imaginary parts of the potential.

The analysis in Fig. 4.3 focuses on the influence of a negative coefficient for the momentum term, Γ, on soliton dynamics. This observation is particularly significant as it highlights the robustness of the soliton solutions, which continue to align

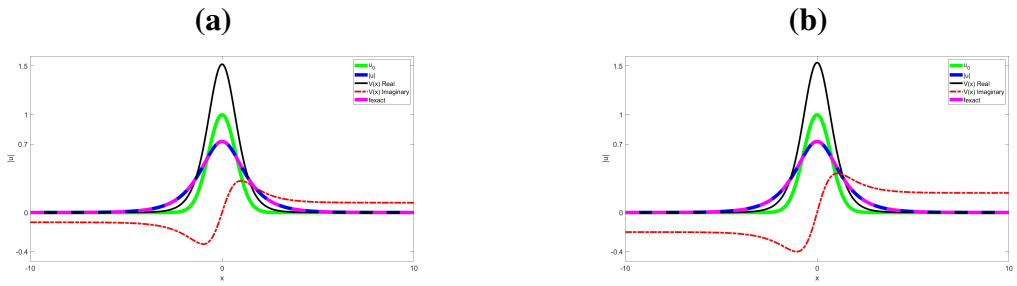

Figure 4.3 : The exact and numerical solutions of the NLS equation for $\mu = 1, W_1 = 0.5, V_2 = 1.5$ when (a) $\Gamma = -0.1$, (b) $\Gamma = -0.2$

with theoretical exact solutions despite the altered parameter regime. The observed reduction in soliton amplitude under negative growth conditions suggests that the system's energy dynamics are sensitive to the sign of Γ potentially influencing the overall stability and behavior of the solitonic structure. Such findings contribute to a deeper understanding of the interplay between parameter variations and soliton stability in nonlinear systems.

In Fig. 4.4, all the obtained solitons are shown for the NLS equation with $\mathscr{P}\mathscr{T}$-symmetric potential and momentum term for varying potential depths V_2-W_1. In this figure, the constraint curve $V_2 = 2 + W_1^2/9$ is depicted by dashed line.

There is no existence on the right side of the curve as the soliton would have no real solution. After marking the regions where solitons exist, it is observed that the existence region narrows with the increment of Γ.

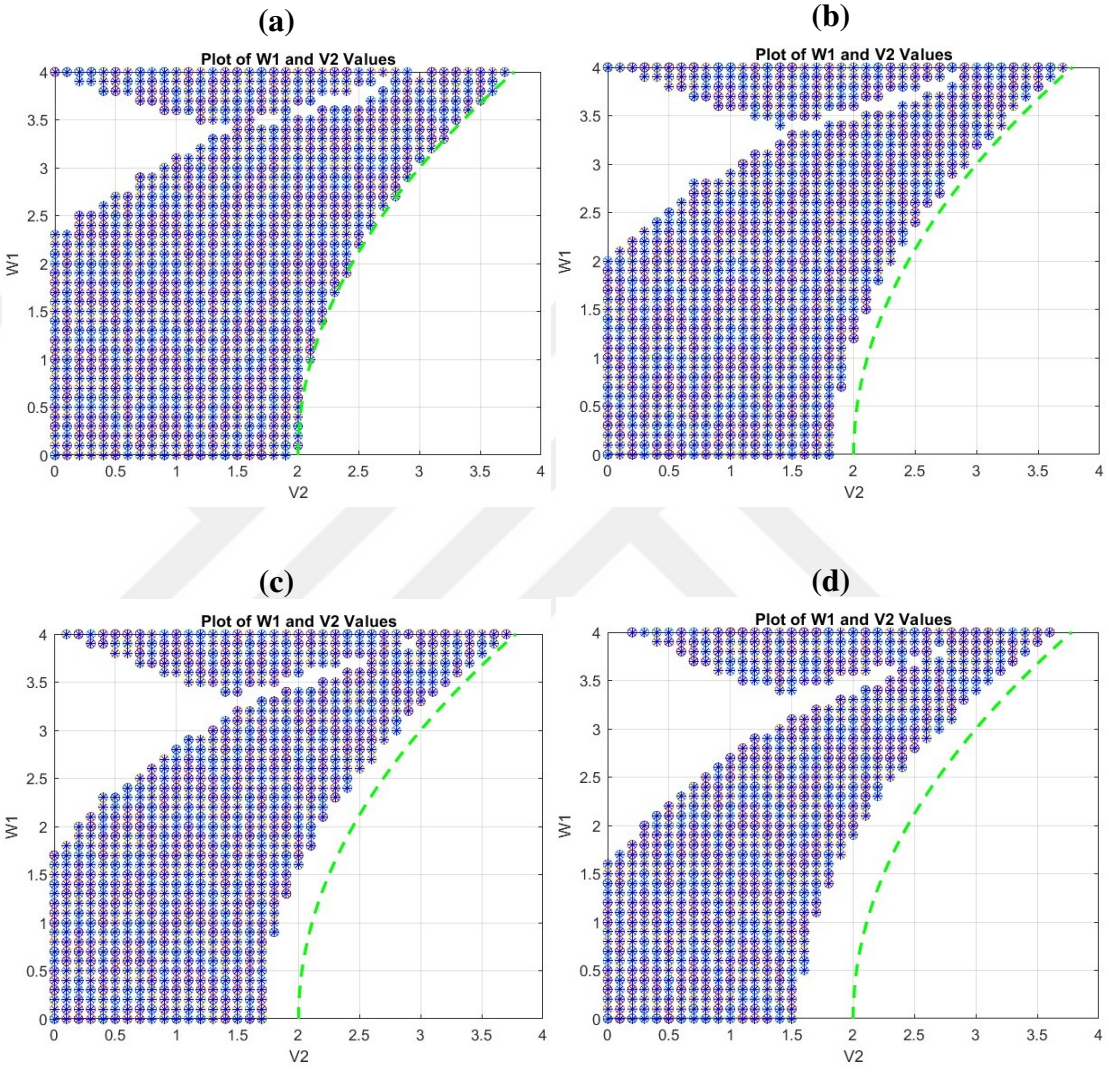

Figure 4.4 : Existence region of the NLS equation with $\mathscr{P}\mathscr{T}$-symmetric potential and momentum term for varying potential depths with $\mu = 1$ and (a) $\Gamma = 0$, (b) $\Gamma = 0.1$, (c) $\Gamma = 0.2$, (d) $\Gamma = 0.3$

5. STABILITY ANALYSIS

5.1 Split-Step Fourier Method

One kind of evolution approach is the Split-step Fourier approach. The Split-step Fourier Method is for solving wave equations [40, 41]. The evolution equation is divided into multiple parts as the basis for the procedure. Although this method's concept dates back a long way, its application to NLS-type equations has only recently come under investigation.

5.2 Nonlinear Stability Analysis

"Nonlinearly stable" in the context of optics refers to a soliton that maintains its maximum amplitude, shape, and position during propagation. The generated solitons will be computed over a long distance in order to study the nonlinear stability. In this thesis, $z = 100$ is sufficient to determine the nonlinear stability of a soliton.

Consider Eq. (1.2) which can be rewritten as

$$u_z = i\alpha u_{xx} + \Gamma u_x + i|u|^2 u + iV_{PT}u, \tag{5.1}$$

and thus can be split as in Eq. (5.1) with the linear operator $M = i(\alpha\partial_{xx} - i\Gamma\partial_x)$ and the operator $N = i(|u|^2 + V_{PT})$. The linear step $u_z = Mu$ is solved with the Fourier transform. Taking the Fourier transform of both sides of

$$u_z = i\alpha u_{xx} + \Gamma u_x \tag{5.2}$$

gives

$$\hat{u}_z = i\alpha(ik_x)^2\hat{u} + \Gamma(ik_x)\hat{u} = -i(\alpha k_x^2 - \Gamma k_x)\hat{u}. \tag{5.3}$$

This is an ordinary differential equation (ODE) of $\hat{u}$ and has an exact solution of

$$\hat{u} = \hat{C}_1 e^{-i(\alpha k_x^2 - \Gamma k_x)z} \Rightarrow u = \mathscr{F}^{-1}\left(\hat{C}_1 e^{-i(\alpha k_x^2 - \Gamma k_x)z}\right). \tag{5.4}$$

The step $u_z = Nu$, i.e.

$$u_z = i(|u|^2 + V_{PT})u \tag{5.5}$$

has the exact solution

$$u = C_2 e^{i(|u|^2 + V_{PT})z}. \tag{5.6}$$

With the answers to both parts obtained, any splitting scheme can be used to apply the Split-Step Fourier technique to the equation in Eq. (1.2).

To investigate the nonlinear stability of solitons, the numerically produced solitons are taken as the initial condition in Split-step Fourier method up to $z = 100$. The solitons are evolved, and the maximum amplitude as a function of the propagation distance z are plotted.

First, to examine the effect of the momentum term on nonlinear stability, an analysis was conducted with various values of Γ in the absence of a potential.

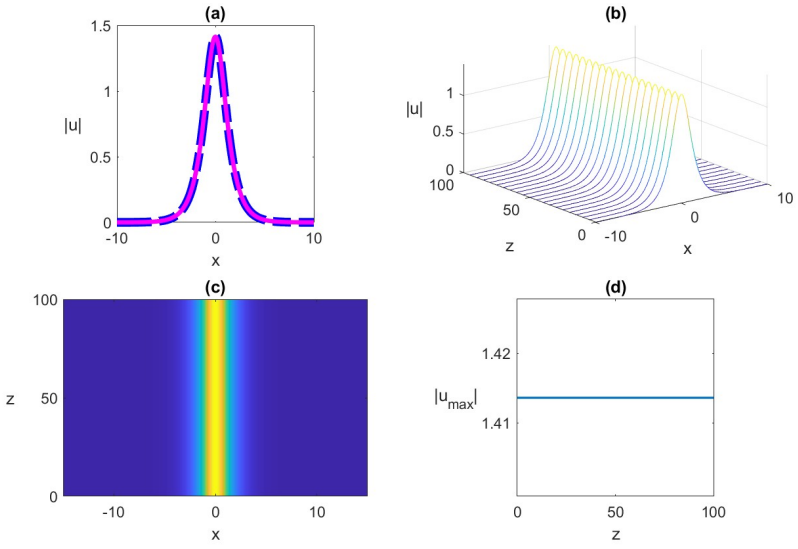

Figure 5.1 : Nonlinear stability of soliton for μ = 1 and $\Gamma = 0$ without an external potential; (a) Numerically produced soliton (blue dashes) and the soliton after the evolution (purple solid), (b) Nonlinear evolution of the soliton, (c) The view from the top and (d) Maximum amplitude as a function of the propagation distance z.

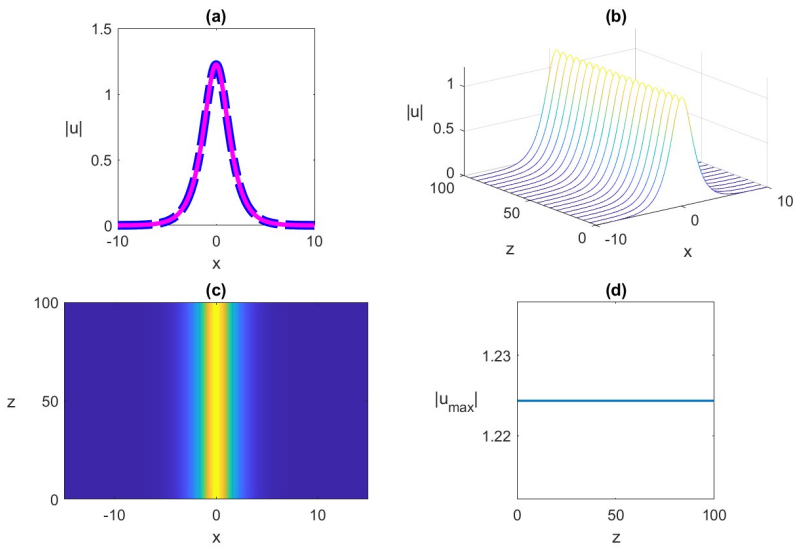

Figure 5.2 : Nonlinear stability for $\mu = 1$ and $\Gamma = 1$ without an external potential; (a) Numerically produced soliton (blue dashes) and the soliton after the evolution (purple solid), (b) Nonlinear evolution of the soliton, (c) The view from the top and (d) Maximum amplitude as a function of the propagation distance z.

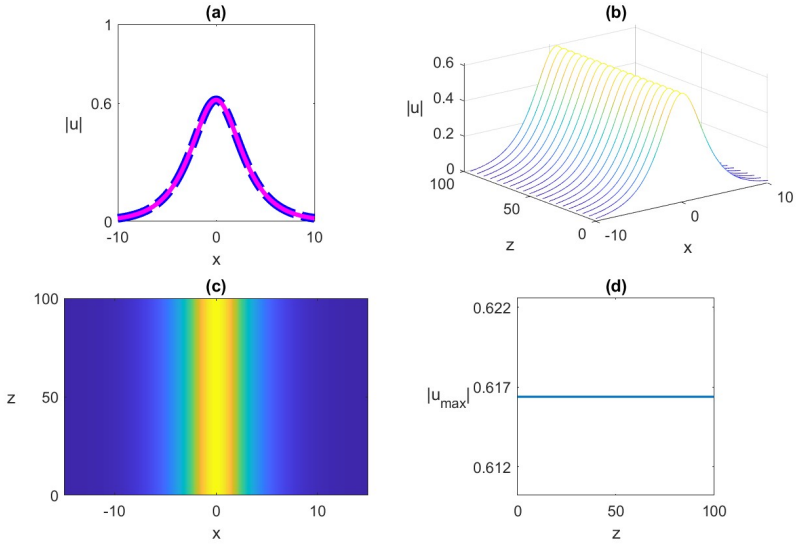

Figure 5.3 : Nonlinear stability for $\mu = 1$ and $\Gamma = 1.8$ without an external potential; (a) Numerically produced soliton (blue dashes) and the soliton after the evolution (purple solid), (b) Nonlinear evolution of the soliton, (c) The view from the top and (d) Maximum amplitude as a function of the propagation distance z.

In Fig. 5.1, the momentum term and potential are both excluded, thus the nonlinear stability of the standart cubic NLS equation has been analyzed. It is observed that the NLS equation exhibits nonlinear stability under these conditions. This implies that the

equation maintains a stable evolution where small perturbations do not grow over time, preserving the overall system configuration and indicating stability.

In Fig. 5.2, the Γ parameter is increased, and $\Gamma = 1$ is considered. The analysis shows that no breakdown of nonlinear stability occurs with this increment in Γ. That is, even with $\Gamma = 1$, the NLS equation remains stable.

In Fig. 5.3, the Γ parameter is further increased to Γ=1.8. The analysis reveals that even with this higher value of Γ, no breakdown of nonlinear stability occurs. This indicates that the NLS equation continues to maintain its stability, demonstrating the robustness of the system against significant increases in the momentum term coefficient.

Furthermore, it is observed in Fig. 5.1, Fig. 5.2 and Fig. 5.3 that as the Γ value increases, the amplitude of solitons decreases. This observation is consistent with the findings from Chapter 3, where a similar conclusion was drawn. The increase in Γ has a direct impact on the behavior of solitons, leading to a decrease in their amplitude.

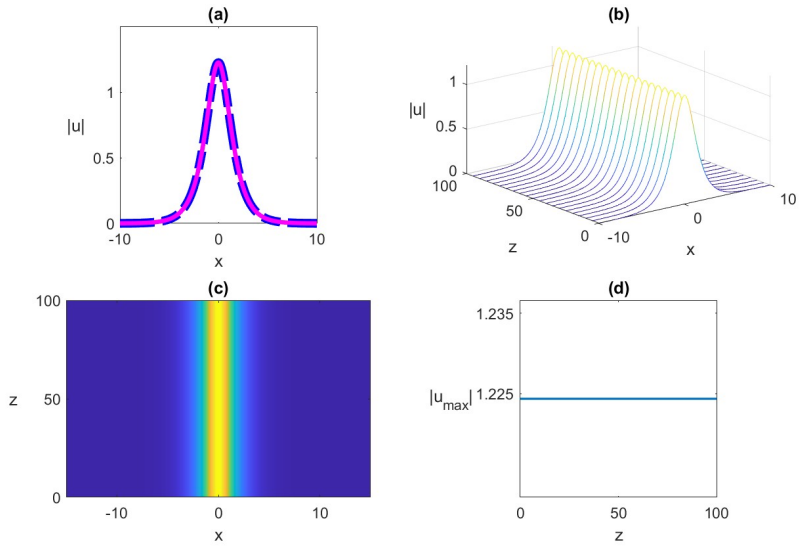

Figure 5.4 : Nonlinear stability for $\mu = 1$ and $\Gamma = -1$ without an external potential; (a) Numerically produced soliton (blue dashes) and the soliton after the evolution (purple solid), (b) Nonlinear evolution of the soliton, (c) The view from the top and (d) Maximum amplitude as a function of the propagation distance z.

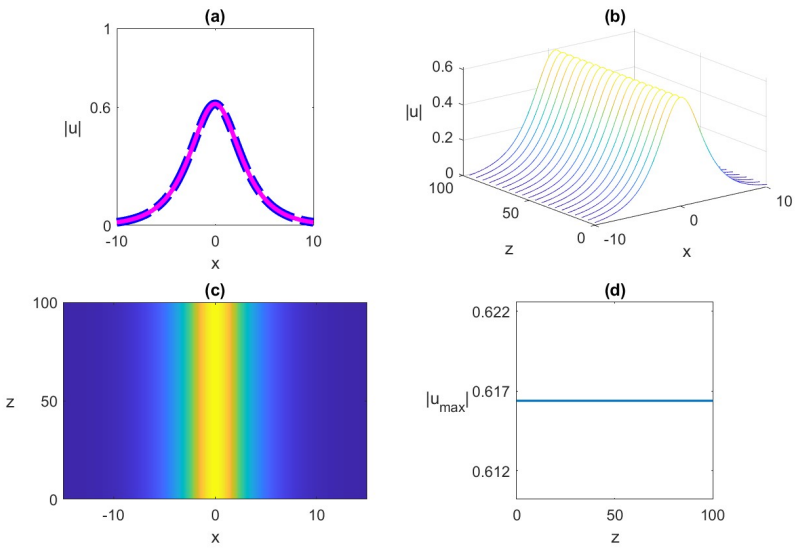

Figure 5.5 : Nonlinear stability for μ = 1 and $\Gamma = -1.8$ without an external potential; (a) Numerically produced soliton (blue dashes) and the soliton after the evolution (purple solid), (b) Nonlinear evolution of the soliton, (c) The view from the top and (d) Maximum amplitude as a function of the propagation distance z.

In Fig. 5.4, the nonlinear stability of the NLS equation is investigated for $\Gamma = -1$. The analysis shows that no breakdown of stability occurs in this negative regime either.

In Fig. 5.5, the parameter Γ is further decreased to $\Gamma = -1.8$. The system remains nonlinearly stable, and the soliton amplitude continues to decrease, again aligning with the findings of Chapter 3. These observations highlight the robustness of the NLS equation against changes in the sign and magnitude of Γ.

After investigating the effects of the momentum term, the nonlinear stability of solitons with the $\mathscr{P}\mathscr{T}$-symmetric potential are investigated without the momentum term. Therefore, $\Gamma = 0$ is set and only the external $\mathscr{P}\mathscr{T}$-symmetric potential in Figures 5.6, 5.7, 5.8 and 5.9 are considered.

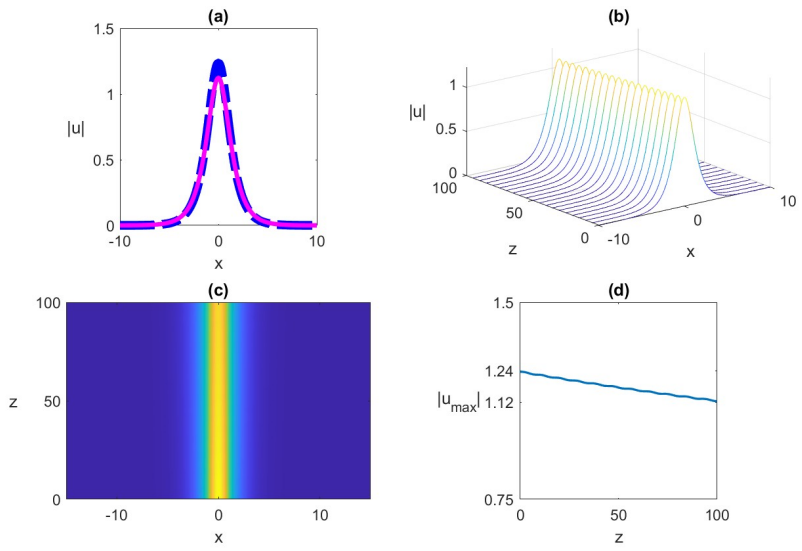

Figure 5.6 : Nonlinear stability for $\mu = 1, \Gamma = 0$ and $W_1 = 0.5, V_2 = 0.5$ with a $\mathscr{P}\mathscr{T}$-symmetric potential; (a) Numerically produced soliton (blue dashes) and the soliton after the evolution (purple solid), (b) Nonlinear evolution of the soliton, (c) The view from the top and (d) Maximum amplitude as a function of the propagation distance z.

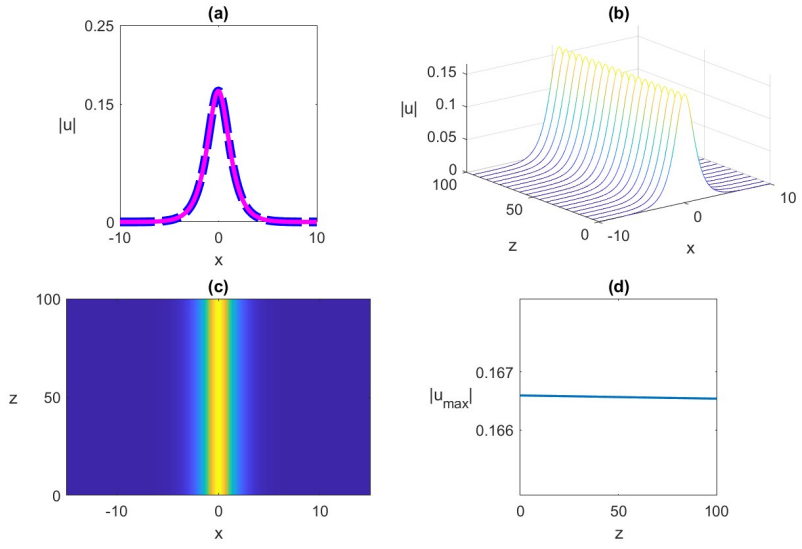

Figure 5.7 : Nonlinear stability for $\mu = 1, \Gamma = 0$ and $W_1 = 0.5, V_2 = 2$ with a $\mathscr{P}\mathscr{T}$-symmetric potential; (a) Numerically produced soliton (blue dashes) and the soliton after the evolution (purple solid), (b) Nonlinear evolution of the soliton, (c) The view from the top and (d) Maximum amplitude as a function of the propagation distance z.

In Fig. 5.6, the Γ parameter is set to $\Gamma = 0$, while the potential depths W_1 and V_2 are both chosen as 0.5. During the evolution, a small oscillation in the maximum amplitude is observed, but the soliton maintains its shape over a long distance ($z = 100$). This

implies that despite the minor oscillations, the soliton remains stable, demonstrating resilience to small perturbations in this parameter regime.

In Fig. 5.7, the real part of the potential depth, V_2, is increased to 2, while W_1 is kept constant at 0.5. The analysis shows that increasing the real part of the potential significantly reduces the soliton amplitude. Interestingly, this reduction in the amplitude coincides with a substantial strengthening of the soliton's nonlinear stability. Hence, increasing the real part of the potential leads to a considerable drop in soliton amplitude, while simultaneously reinforcing the system's overall stability. This suggests that as the depth of the real part of the potential increases, the solitons become more robust.

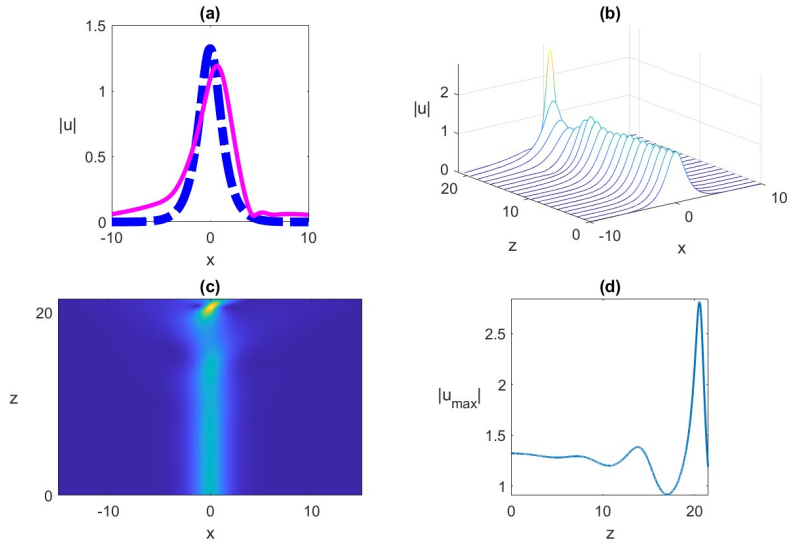

Figure 5.8 : Nonlinear instability for $\mu = 1, \Gamma = 0$ and $W_1 = 1.5, V_2 = 0.5$ with a $\mathscr{P}\mathscr{T}$-symmetric potential; (a) Numerically produced soliton (blue dashes) and the soliton after the evolution (purple solid), (b) Nonlinear evolution of the soliton, (c) The view from the top and (d) Maximum amplitude as a function of the propagation distance z.

In Fig. 5.8, the real part of the potential depth V_2, is fixed at 0.5 and the depth of the complex part of the potential W_1 is increased, and set to $W_1 = 1.5$. This setup explores the impact of increasing the depth of the complex potential while keeping the real part small. From the figure, it is observed that the maximum amplitude start to fluctuate just after $z \approx 10$ and makes a sharp peak at $z = 20$ leading to nonlinear instability. It is also shown that the shape of the soliton is deteriorated. This indicates that increasing the depth of the complex potential while keeping the real part small leads instability of solitons due to the sharp increment.

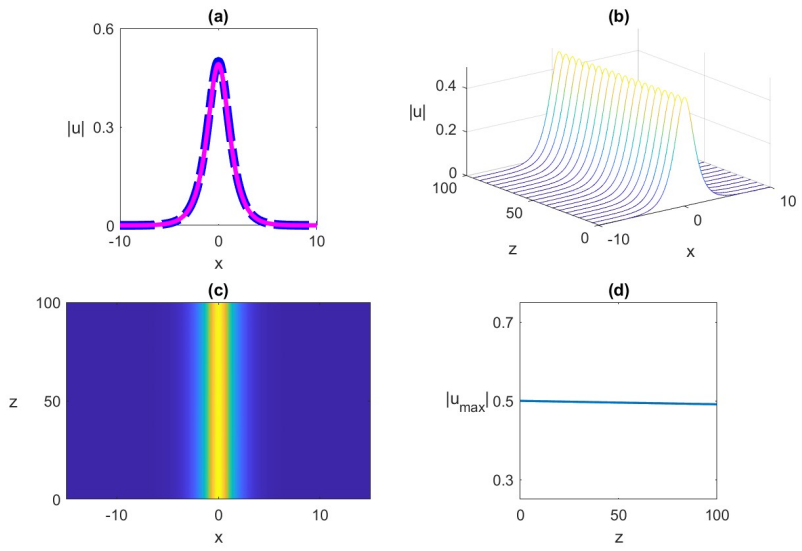

Figure 5.9 : Nonlinear stability for $\mu = 1$, $\Gamma = 0$ and $W_1 = 1.5, V_2 = 2$ with a $\mathscr{P}\mathscr{T}$-symmetric potential; (a) Numerically produced soliton (blue dashes) and the soliton after the evolution (purple solid), (b) Nonlinear evolution of the soliton, (c) The view from the top and (d) Maximum amplitude as a function of the propagation distance z.

In Fig. 5.9, to balance this instability, the complex part of the potential depth $W_1 = 1.5$ is fixed, while the real part of the potential depth is increased to $V_2 = 2$. The analysis shows that when the depth of the real part of the potential is sufficiently large, it compensates for the instability caused by the complex part. This occurs at the cost of a significant reduction in the soliton's amplitude, but nonetheless, the soliton regains its stability. Therefore, increasing the depth of the real part of the potential to an adequate level restores the system's stability and allows the soliton to maintain its nonlinear stability.

In order to examine the effects of both the $\mathscr{P}\mathscr{T}$-symmetric potential and the momentum term, the coefficient of the momentum term, Γ is taken as $\Gamma = 0.1$. In Fig. 5.10, the potential depths are kept small, with $W_1 = 0.5$ and $V_2 = 0.5$, while $\Gamma = 0.1$ is chosen. In previous cases where no potential was present, the momentum term in the NLS equation always preserved stability. However, in this case, even with a small $\Gamma = 0.1$, the inclusion of the potential causes significant oscillations in the soliton as it propagates along the z-axis, reaching 100 units. While the soliton can still be considered nonlinear stable, it is predicted that the wave will eventually break down and disperse after further propagation. This shows that even a small increase in Γ brings the effect of the potential into play, influencing the soliton's behavior.

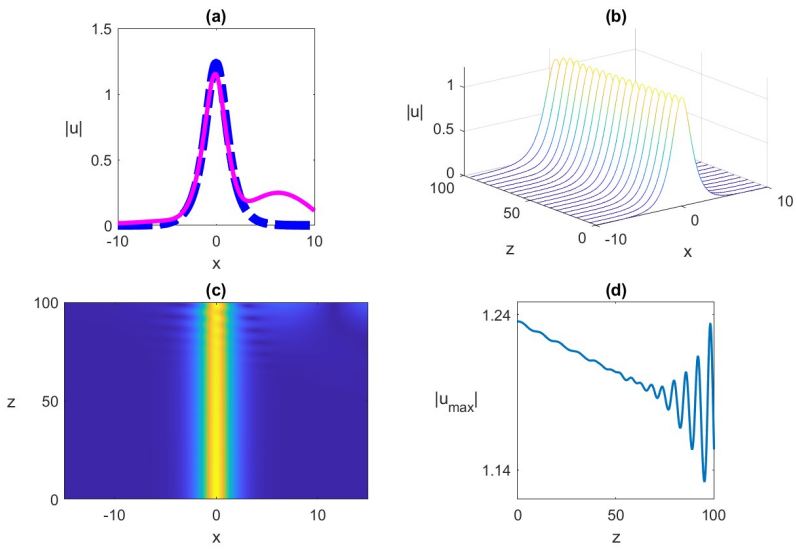

Figure 5.10 : Nonlinear instability for $\mu = 1$, $\Gamma = 0.1$ and $W_1 = 0.5, V_2 = 0.5$ with a $\mathscr{P}\mathscr{T}$-symmetric potential; (a) Numerically produced soliton (blue dashes) and the soliton after the evolution (purple solid), (b) Nonlinear evolution of the soliton, (c) The view from the top and (d) Maximum amplitude as a function of the propagation distance z.

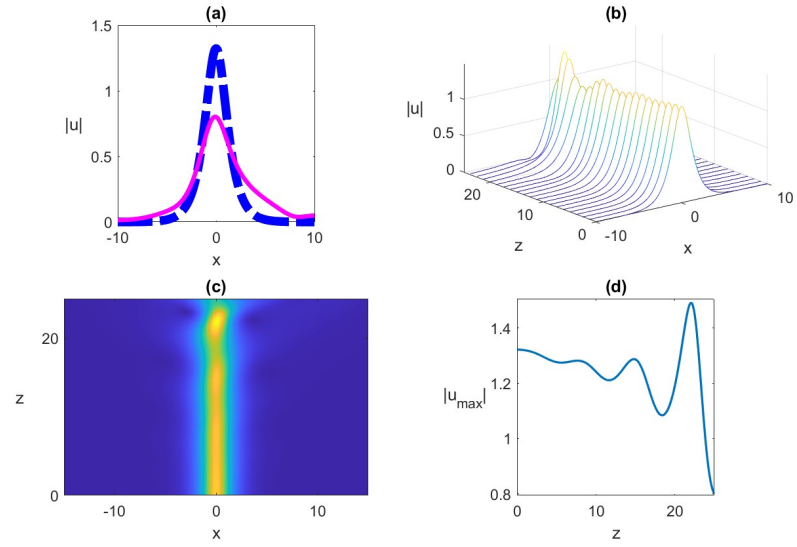

Figure 5.11 : Nonlinear instability for $\mu = 1$, $\Gamma = 0.1$ and $W_1 = 1.5, V_2 = 0.5$ with a $\mathscr{P}\mathscr{T}$-symmetric potential; (a) Numerically produced soliton (blue dashes) and the soliton after the evolution (purple solid), (b) Nonlinear evolution of the soliton, (c) The view from the top and (d) Maximum amplitude as a function of the propagation distance z.

In Fig. 5.11, the values of Γ and the real potential depth V_2 are kept the same, but the complex part of the potential depth W_1 is increased to $W_1 = 1.5$. Previous analyses showed that increasing the depth of the complex part of the potential destabilizes the soliton. It is observed that even with $\Gamma = 0.1$, this increase in W_1 causes the soliton's

shape to break down before reaching 20 units along the z-axis, leading the soliton to instability. This further confirms that, despite the small value of Γ, increasing the complex potential depth disrupts the stability of the soliton and causes the system to lose its stability.

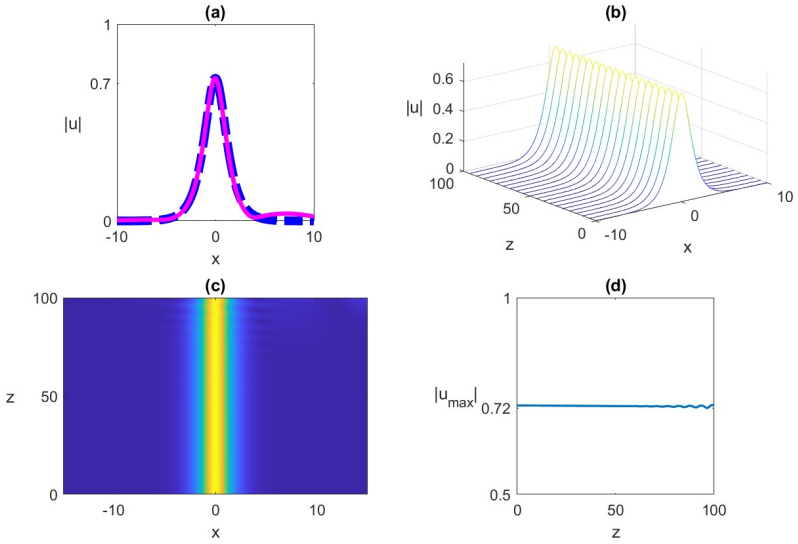

Figure 5.12 : Nonlinear stability for $\mu = 1$, $\Gamma = 0.1$ and $W_1 = 0.5, V_2 = 1.5$ with a $\mathscr{P}\mathscr{T}$-symmetric potential; (a) Numerically produced soliton (blue dashes) and the soliton after the evolution (purple solid), (b) Nonlinear evolution of the soliton, (c) The view from the top and (d) Maximum amplitude as a function of the propagation distance z.

In Fig. 5.12, the depth of the complex part of the potential, W_1 is kept at 0.5, while the depth of the real part, V_2 is increased to $V_2 = 1.5$. As predicted from previous analyses, increasing the real part of the potential, even with $\Gamma = 0.1$, results in only very small visible oscillations. However, these small oscillations do not destabilize the soliton, and it remains nonlinear stable. This shows that the increase in the real potential depth enhances the stability of the soliton despite the small oscillations caused by the non-zero Γ value.

In Fig. 5.13, the potential depths $W_1 = 0.5$ and $V_2 = 1.5$ are kept the same as in the previous figure, but the Γ parameter is increased to $\Gamma = 0.2$. This small change in Γ immediately causes a noticeable destabilization of the soliton. Observations show that as the soliton propagates beyond 50 units along the z-axis, its structure breaks down, and it becomes nonlinear unstable. Despite having chosen a small complex potential depth and a large real potential depth to stay within the existence region, the increase in Γ to 0.2 makes the soliton nonlinear unstable. This finding indicates that

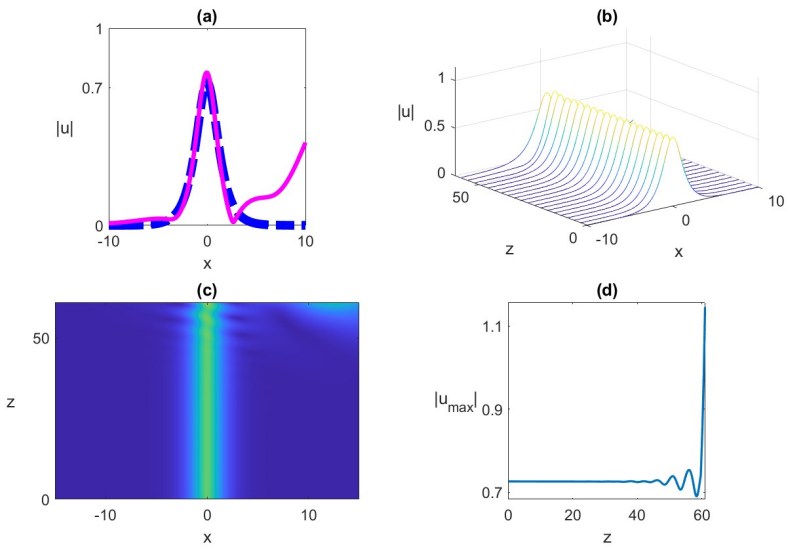

Figure 5.13 : Nonlinear instability for $\mu = 1$, $\Gamma = 0.2$ and $W_1 = 0.5, V_2 = 1.5$ with a $\mathscr{P}\mathscr{T}$-symmetric potential; (a) Numerically produced soliton (blue dashes) and the soliton after the evolution (purple solid), (b) Nonlinear evolution of the soliton, (c) The view from the top and (d) Maximum amplitude as a function of the propagation distance z.

the $\mathscr{P}\mathscr{T}$-symmetric potential and momentum-term NLS equation becomes nonlinear unstable for Γ values greater than 0.1, regardless of the chosen potential depths.

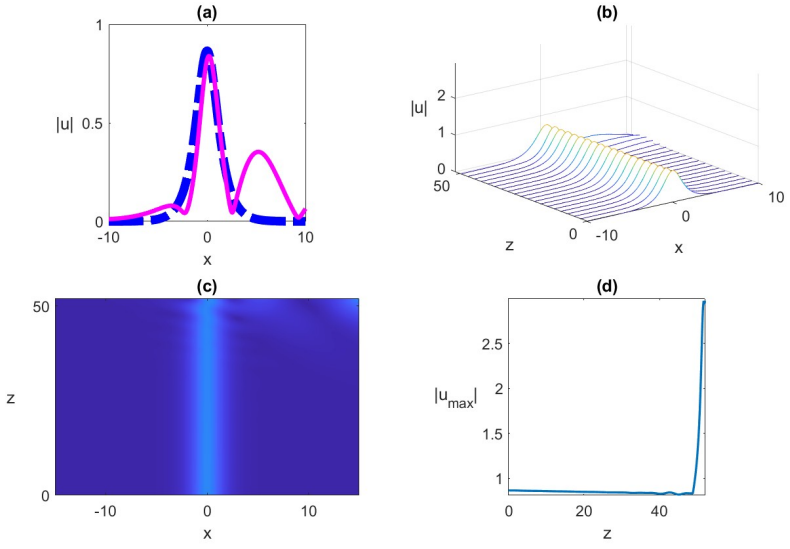

Figure 5.14 : Nonlinear instability for $\mu = 1$, $\Gamma = 0.2$ and $W_1 = 1.5, V_2 = 1.5$ with a $\mathscr{P}\mathscr{T}$-symmetric potential; (a) Numerically produced soliton (blue dashes) and the soliton after the evolution (purple solid), (b) Nonlinear evolution of the soliton, (c) The view from the top and (d) Maximum amplitude as a function of the propagation distance z.

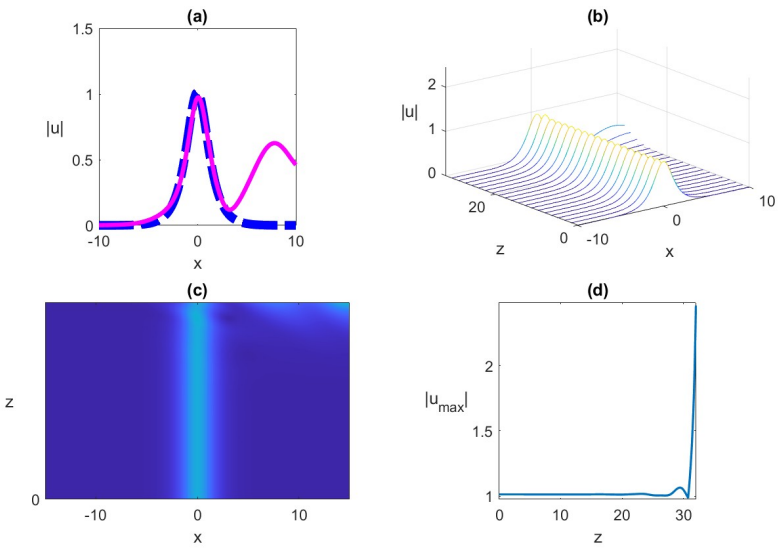

Figure 5.15 : Nonlinear instability for $\mu = 1$, $\Gamma = 0.4$ and $W_1 = 0.5, V_2 = 1$ with a $\mathscr{P}\mathscr{T}$-symmetric potential; (a) Numerically produced soliton (blue dashes) and the soliton after the evolution (purple solid), (b) Nonlinear evolution of the soliton, (c) The view from the top and (d) Maximum amplitude as a function of the propagation distance z.

In Fig. 5.14, the depth of the complex part of the potential, W_1, is increased to 1.5, and the soliton's structure is analyzed once again for $\Gamma = 0.2$. As expected, the increase in the complex potential depth does not restore the soliton's stability. The soliton remains nonlinearly unstable, unable to regain its stability. This result highlights how the system's stability rapidly deteriorates with the increment in the complex potential depth, even under a relatively small value of Γ, indicating that the soliton cannot maintain its stability in such conditions.

In Fig. 5.15, the Γ value is doubled once more, reaching $\Gamma = 0.4$. The potential depth values are chosen within the existence region, with $W_1 = 0.5$ and $V_2 = 1$. Previous analyses showed that increasing Γ plays a detrimental role in the soliton's stability, and a similar pattern is observed here. With $\Gamma = 0.4$, despite selecting a small complex potential depth and a relatively larger real potential depth, the soliton is unable to propagate beyond 30 units along the z-axis before its structure breaks down, rendering it nonlinear unstable. This result further demonstrates that increasing Γ to 0.4 significantly destabilizes the system, preventing the soliton from maintaining its nonlinear stability.

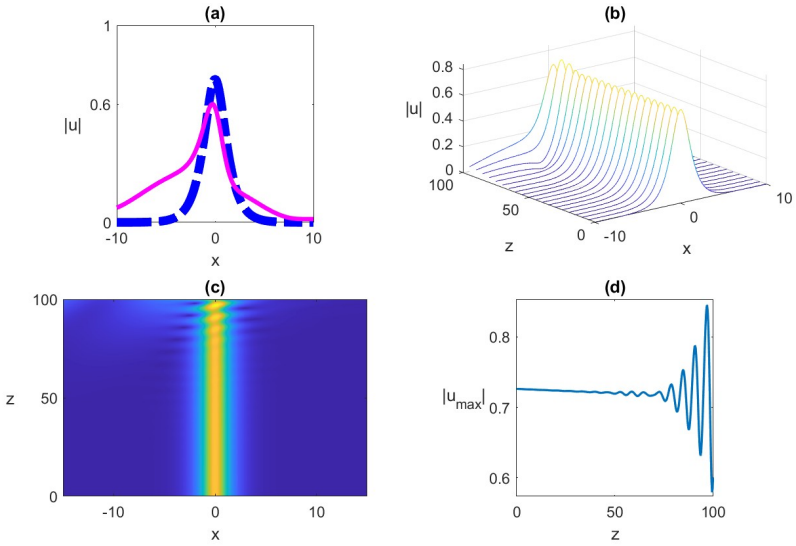

Figure 5.16 : Nonlinear instability for $\mu = 1, \Gamma = -0.1$ and $W_1 = 0.5, V_2 = 1.5$ with a $\mathscr{P}\mathscr{T}$-symmetric potential; (a) Numerically produced soliton (blue dashes) and the soliton after the evolution (purple solid), (b) Nonlinear evolution of the soliton, (c) The view from the top and (d) Maximum amplitude as a function of the propagation distance z.

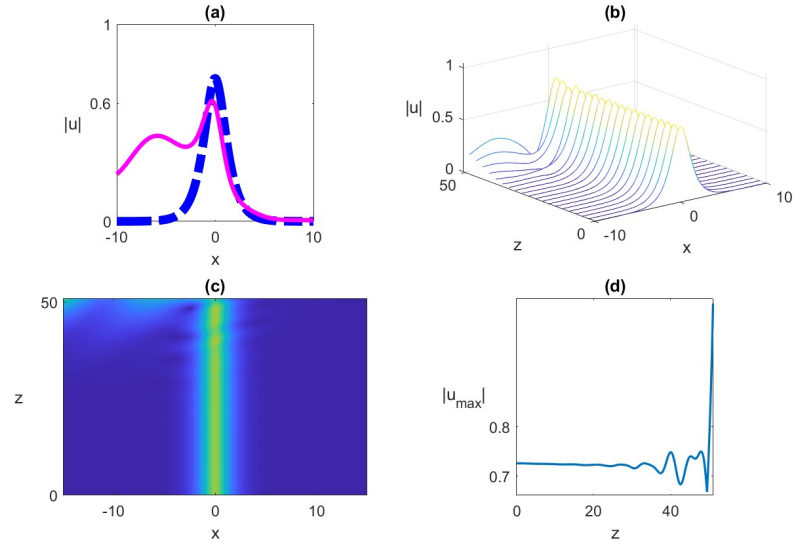

Figure 5.17 : Nonlinear instability for $\mu = 1, \Gamma = -0.2$ and $W_1 = 0.5, V_2 = 1.5$ with a $\mathscr{P}\mathscr{T}$-symmetric potential; (a) Numerically produced soliton (blue dashes) and the soliton after the evolution (purple solid), (b) Nonlinear evolution of the soliton, (c) The view from the top and (d) Maximum amplitude as a function of the propagation distance z.

In Fig. 5.16, the system is examined for $\Gamma = -0.1$ under the conditions $W_1 = 0.5$ and $V_2 = 1.5$. The results reveal that, for this slightly negative Γ, the evolution deteriorates

faster compared to positive Γ, though the soliton shape remains relatively stable for longer durations compared to lower negative values for Γ.

In Fig. 5.17, $\Gamma = -0.2$ is considered with the same potential depth settings. It is observed that the soliton begins to lose its shape around $z \approx 45$, whereas for $\Gamma = 0.2$, the soliton persists until approximately $z \approx 60$ under similar conditions. These findings highlight the increased sensitivity of soliton evolutions to the sign of Γ, particularly when Γ is negative.

All these analyses demonstrated that with the $\mathscr{P}\mathscr{T}$-symmetric potential and the momentum term, NLS equation loses the nonlinear stability of solitons with increasing values of Γ, and the preservation of stability depends on the careful adjustment of potential depths. Even at small values of Γ, an increase in the complex part of the potential can cause nonlinear instability of the soliton.

5.3 Linear Stability

By obtaining and examining the linear spectra of the produced solitons, linear stability will be examined.

5.3.1 Linear spectrum

The eigenvalues of a soliton's linear stability operator are known as the linear stability spectrum, or simply the linear spectrum. These eigenvalues provide details regarding a soliton's linear stability properties. Consider the following equation, which contains nonlinearities of a general kind where $F(\cdot) \in \mathbb{R}$ and $F(0) = 0$:

$$iu_z(x,z) + \alpha u_{xx}(x,z) - i\Gamma u_x(x,z) + F\left(|u(x,z)|^2\right) u(x,z) + V_{PT}(x)u(x,z) = 0. \quad (5.7)$$

Eq. (5.7) accepts soliton solutions of the form $u(x,z) = f(x)e^{i\mu z}$. Substituting

$$\begin{aligned} u_z &= i\mu f e^{i\mu z} \\ u_x &= f_x e^{i\mu z} \\ u_{xx} &= f_{xx} e^{i\mu z} \\ |u|^2 &= uu^* = f e^{i\mu z} f^* e^{-i\mu z} = ff^* = |f|^2 \end{aligned} \quad (5.8)$$

in Eq. (5.7) and multiplying by $e^{-i\mu z}$ gives

$$-\mu f + \alpha f_{xx} - i\Gamma f_x + F(|f|^2)f + V_{PT} f = 0. \quad (5.9)$$

The soliton solution is perturbed in the following ways in order to analyze the linear stability:

$$u(x,z) = [f(x) + g(x)e^{\sigma z} + h^*(x)e^{\sigma^* z}]e^{i\mu z}, \tag{5.10}$$

where g and h are perturbation eigenfunctions and σ is the eigenvalue.

$$\begin{aligned} u_z &= \left(\sigma g e^{\sigma z} + \sigma^* h^* e^{\sigma^* z} + i\mu f + i\mu g e^{\sigma z} + i\mu h^* e^{\sigma^* z}\right) e^{i\mu z} \\ u_x &= \left(f_x + g_x e^{\sigma z} + h_x^* e^{\sigma^* z}\right) e^{i\mu z} \\ u_{xx} &= \left(f_{xx} + g_{xx} e^{\sigma z} + h_{xx}^* e^{\sigma^* z}\right) e^{i\mu z}, \end{aligned} \tag{5.11}$$

and $|u|^2$ is calculated as

$$\begin{aligned} |u|^2 &= \left(f + g e^{\sigma z} + h^* e^{\sigma^* z}\right) e^{i\mu z} \left(f^* + g^* e^{\sigma^* z} + h e^{\sigma z}\right) e^{-i\mu z} \\ &= |f|^2 + f g^* e^{\sigma^* z} + f^* g e^{\sigma z} + |g|^2 e^{(\sigma+\sigma^*)z} + f h e^{\sigma z} \\ &\quad + f^* h^* e^{\sigma^* z} + g^* h^* e^{2\sigma^* z} + g h e^{2\sigma z} + |h|^2 e^{(\sigma+\sigma^*)z} \\ &\cong |f|^2 + (g^* e^{\sigma^* z} + h e^{\sigma z}) f + (g e^{\sigma z} + h^* e^{\sigma^* z}) f^*. \end{aligned} \tag{5.12}$$

Using linear Taylor expansion $F(x+h) = F(x) + hF'(x) + O(h^2)$,

$$\begin{aligned} F(|u|^2) &= F\left(|f|^2 + h\left(g^* e^{\sigma^* z} + h e^{\sigma z}\right) f + \left(g e^{\sigma z} + h^* e^{\sigma^* z}\right) f^*\right) \\ &\cong F(|f|^2) + \left[\left(g^* e^{\sigma^* z} + h e^{\sigma z}\right) f + \left(g e^{\sigma z} + h^* e^{\sigma^* z}\right) f^*\right] F'(|f|^2). \end{aligned} \tag{5.13}$$

Thus,

$$\begin{aligned} & F(|u|^2) u e^{-i\mu z} \\ &= F(|f|^2) + \left[\left(g^* e^{\sigma^* z} + h e^{\sigma z}\right) f^2 + \left(g e^{\sigma z} + h^* e^{\sigma^* z}\right) |f|^2\right] F'(|f|^2) \\ &+ F(|f|^2) g e^{\sigma z} + F(|f|^2) h^* e^{\sigma^* z} \\ &+ \left[\left(g g^* e^{(\sigma+\sigma^*)z} + g h e^{2\sigma z}\right) f + \left(g^2 e^{2\sigma z} + g h^* e^{(\sigma+\sigma^*)z}\right) f^*\right] F'(|f|^2) \\ &+ \left[\left(g^* h^* e^{2\sigma^* z} + |h|^2 e^{(\sigma+\sigma^*)z}\right) f + \left(g h^* e^{(\sigma+\sigma^*)z} + (h^*)^2 e^{2\sigma^* z}\right) f^*\right] F'(|f|^2) \\ &\cong F'(|f|^2) \left[f + g e^{\sigma z} + h^* e^{\sigma^* z}\right] \\ &+ F'(|f|^2) \left[\left(f^2 h + |f|^2 g\right) e^{\sigma z} + \left(f^2 g^* + |f|^2 h^*\right) e^{\sigma^* z}\right]. \end{aligned} \tag{5.14}$$

Substituting Eq. (5.10), (5.11) and (5.14) into Eq. (5.7) gives

$$\begin{aligned} & i\left(\sigma g e^{\sigma z} + \sigma^* h^* e^{\sigma^* z} + i\mu f + i\mu g e^{\sigma z} + i\mu h^* e^{\sigma^* z}\right) e^{i\mu z} \\ &+ \alpha\left(f_{xx} + g_{xx} e^{\sigma z} + h_{xx}^* e^{\sigma^* z}\right) e^{i\mu z} \\ &- i\Gamma\left(f_x + g_x e^{\sigma z} + h_x^* e^{\sigma^* z}\right) e^{i\mu z} \\ &+ [F(|f|^2)\left[f + g e^{\sigma z} + h^* e^{\sigma^* z}\right] \\ &+ F'(|f|^2)\left(f^2 h + |f|^2 g\right) e^{\sigma z} + \left(f^2 g^* + |f|^2 h^*\right) e^{\sigma^* z}] e^{i\mu z} \\ &+ V_{PT}\left(f + g e^{\sigma z} + h^* e^{\sigma^* z}\right) e^{i\mu z} = 0. \end{aligned} \tag{5.15}$$

Grouping the terms and multiplying by $e^{i\mu z}$ yields

$$\begin{aligned}
&\left[-\mu f+\alpha f_{xx}-i\Gamma f_x+F(|f|^2)f+V_{PT}f\right]\\
&+\left[i\sigma g-\mu g+\alpha g_{xx}-i\Gamma g_x+F(|f|^2)g+\left(f^2h+|f|^2g\right)F'(|f|^2)+V_{PT}g\right]e^{\sigma z}\\
&+\left[i\sigma^* h^*-\mu h^*+\alpha h^*_{xx}-i\Gamma h^*_x+F(|f|^2)h^*+\left(f^2g^*+|f|^2h^*\right)F'(|f|^2)+V_{PT}h^*\right]e^{\sigma^* z}=0.
\end{aligned} \tag{5.16}$$

Since f is a solution seen in Eq. (5.9), the first bracket is identically zero. The elements of the exponentials must both be zero at the same time for Eq. (5.16). Therefore, one has one hand

$$i\sigma g-\mu g+\alpha g_{xx}-i\Gamma g_x+F(|f|^2)g+\left(f^2h+|f|^2g\right)F'(|f|^2)+V_{PT}g=0, \tag{5.17}$$

which can be rewritten as

$$\alpha g_{xx}-i\Gamma g_x+\left[F(|f|^2)+F'(|f|^2)|f|^2-\mu+V_{PT}\right]g+F'(|f|^2)f^2h=-i\sigma g. \tag{5.18}$$

and on the other hand

$$\begin{aligned}
&i\sigma^* h^*-\mu h^*+\alpha h^*_{xx}-i\Gamma h^*_x+F(|f|^2)h^*\\
&+\left(f^2g^*+|f|^2h^*\right)F'(|f|^2)+V_{PT}h^*=0,
\end{aligned} \tag{5.19}$$

which can be rewritten as

$$\begin{aligned}
&\alpha h^*_{xx}-i\Gamma h^*_x+\left[F(|f|^2)+F'(|f|^2)|f|^2-\mu+V_{PT}\right]h^*\\
&+F'(|f|^2)f^2g^*=-i\sigma^* h^*.
\end{aligned} \tag{5.20}$$

Taking the conjugate of Eq. (5.20) gives

$$\begin{aligned}
&\alpha h_{xx}-i\Gamma h_x+\left[F(|f|^2)+F'(|f|^2)|f|^2-\mu+V^*_{PT}\right]h\\
&+F'(|f|^2)(f^2)^*g=i\sigma h.
\end{aligned} \tag{5.21}$$

Multiplying Eq. (5.21) by -1 gives

$$\begin{aligned}
&-\alpha h_{xx}+i\Gamma h_x-\left[F(|f|^2)+F'(|f|^2)|f|^2-\mu+V^*_{PT}\right]h\\
&-F'(|f|^2)(f^2)^*g=-i\sigma h.
\end{aligned} \tag{5.22}$$

Writing Eq. (5.18) and (5.22) in matrix form yields

$$i\begin{pmatrix}L_1 & L_2\\ -L_2^* & -L_1^*\end{pmatrix}\begin{pmatrix}g\\ h\end{pmatrix}=\sigma\begin{pmatrix}g\\ h\end{pmatrix}, \tag{5.23}$$

where

$$\begin{aligned}
L_1&=\alpha\partial_{xx}-i\Gamma\partial_x+F(|f|^2)+F'(|f|^2)|f|^2-\mu+V_{PT}\\
L_2&=F'(|f|^2)f^2.
\end{aligned} \tag{5.24}$$

For the cubic nonlinearity,

$$\begin{aligned} F(x) &= Ax, \\ F'(x) &= A. \end{aligned} \tag{5.25}$$

Using Eq. (5.25) in Eq. (5.24) gives

$$\begin{aligned} L_1 &= \alpha\partial_{xx} - i\Gamma\partial_x + 2A|f|^2 - \mu + V_{PT}, \\ L_2 &= Af^2. \end{aligned} \tag{5.26}$$

If the soliton is real, Eq. (5.26) becomes

$$\begin{aligned} L_1 &= \alpha\partial_{xx} - i\Gamma\partial_x + 2Af^2 - \mu + V_{PT}, \\ L_2 &= Af^2. \end{aligned} \tag{5.27}$$

For different values of Γ, the linear spectrum of numerically produced solitons is found to investigate the effect of the momentum term on the linear stability of the solitons of Eq. (1.2). To investigate the linear stability, it is necessary to examine whether the computed eigenvalues, λ have positive real parts. If there are no positive real parts, the soliton is considered linearly stable.

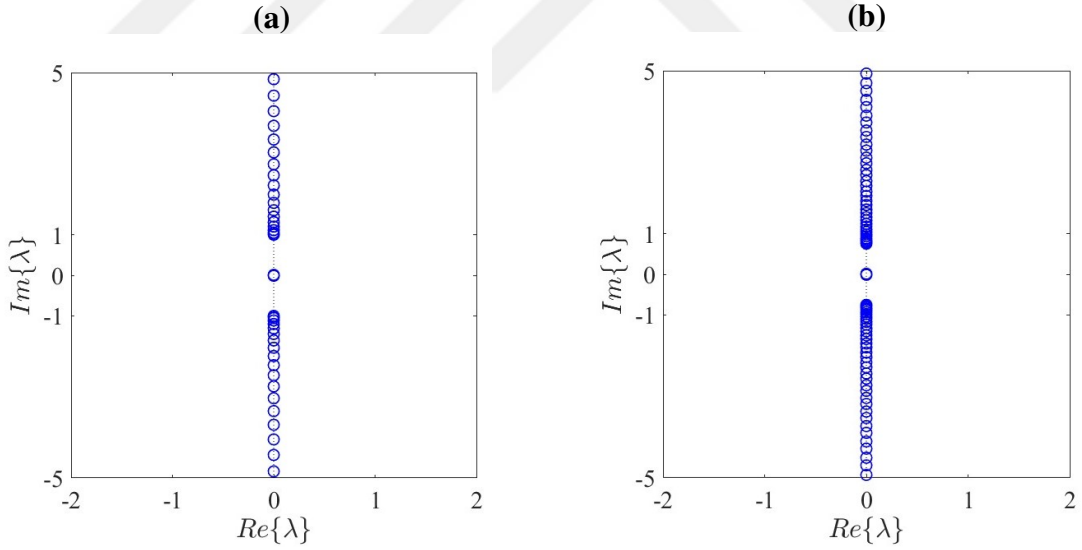

Figure 5.18 : Linear spectra of NLS equation for $\mu = 1$ without an external potential; (a) $\Gamma = 0$, (b) $\Gamma = 1$

In Fig. 5.18, the linear spectra with and without a momentum term are shown. Both cases are studied without any external potential. In Fig. 5.18(a), it is observed that the NLS equation without a momentum term is linearly stable as a result of all pure imaginary eigenvalues.

In Fig. 5.18(b), when the momentum is included, namely taken as $\Gamma = 1$, the number of eigenvalues increase. However, this does not affect the linear stability, as no real parts exist to these eigenvalues. This result shows that even under the influence of the momentum term, the NLS equation maintains its linear stability. Consistent with previous analyses of nonlinear stability, NLS equation is both nonlinearly and linearly stable, demonstrating the robustness of the soliton's stability even at larger values of the momentum term.

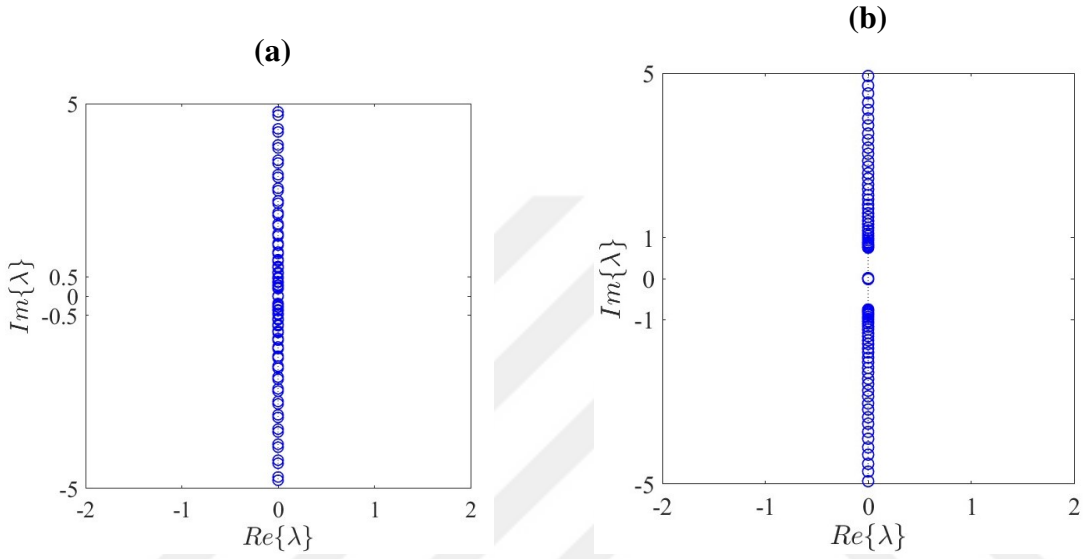

Figure 5.19 : Linear spectra of NLS equation for $\mu = 1$ without an external potential; (a) $\Gamma = -1.8$, (b) $\Gamma = -1$

In Fig. 5.19, the linear spectra for the NLS equation are studied without any external potential, considering $\Gamma = -1.8$ on Fig. 5.19(a) and $\Gamma = -1$ on Fig. 5.19(b).

In Fig. 5.19(a), for $\Gamma = -1.8$, it is observed that the eigenvalues become more densely distributed as the magnitude of Γ increases. However, no real parts exist for these eigenvalues, indicating that the system remains linearly stable. This result is consistent with prior nonlinear stability findings and confirms that the NLS equation retains its robustness under significant negative momentum contributions.

In Fig. 5.19(b), where $\Gamma = -1$, a similar trend of eigenvalue clustering is seen. The absence of real eigenvalues ensures linear stability, highlighting the continued resilience of the NLS equation. These results demonstrate that the equation remains both linearly and nonlinearly stable across a range of negative Γ values, when no external potential is present.

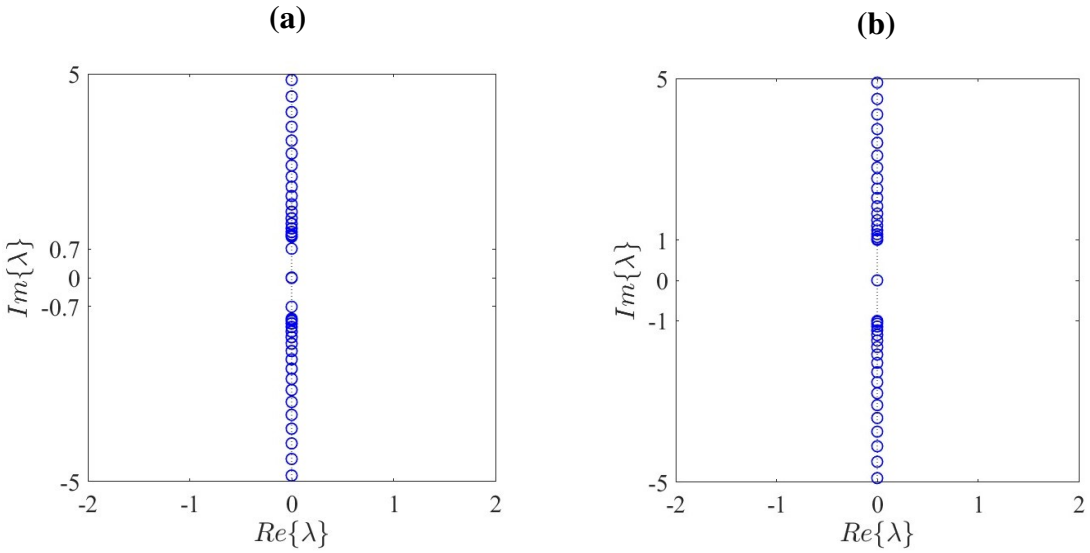

Figure 5.20 : Linear spectra of NLS equation for $\mu = 1, \Gamma = 0$ with a $\mathscr{P}\mathscr{T}$-symmetric potential; (a) $W_1 = 0.5, V_2 = 0.5$, (b) $W_1 = 0.5, V_2 = 2$

In Fig. 5.20, the effect of the $\mathscr{P}\mathscr{T}$-symmetric potential on the linear stability is examined without momentum term. The potential depths are initially chosen as small values for both the real and complex parts, and then the real part is increased. In these analyses, the solitons were found to be nonlinearly stable, and in both cases, they also retained their linear stability.

These results show that, even as the real part of the potential increases, the solitons remain both nonlinearly and linearly stable. The $\mathscr{P}\mathscr{T}$-symmetric potential, even with small depths and an increased real part, does not have a negative impact on the linear stability of the solitons.

In Fig. 5.21, the complex depth of the potential is increased to $W_2 = 1.5$. In Fig. 5.21(a), when the depth of the real part of the potential is fixed at $V_2 = 0.5$, it is found that, similar to the nonlinear stability analysis where the soliton was unstable, the soliton is also linearly unstable, with eigenvalues showing positive real parts.

In Fig. 5.21(b), by increasing the real potential depth to $V_2 = 2.0$, this instability is resolved, and the soliton becomes linearly stable. These results show that the real part of the potential plays a critical role in stabilizing the system. While an increase in the complex depth may lead to instability, sufficient enhancement of the real depth can counteract this effect and restore the soliton's linear stability.

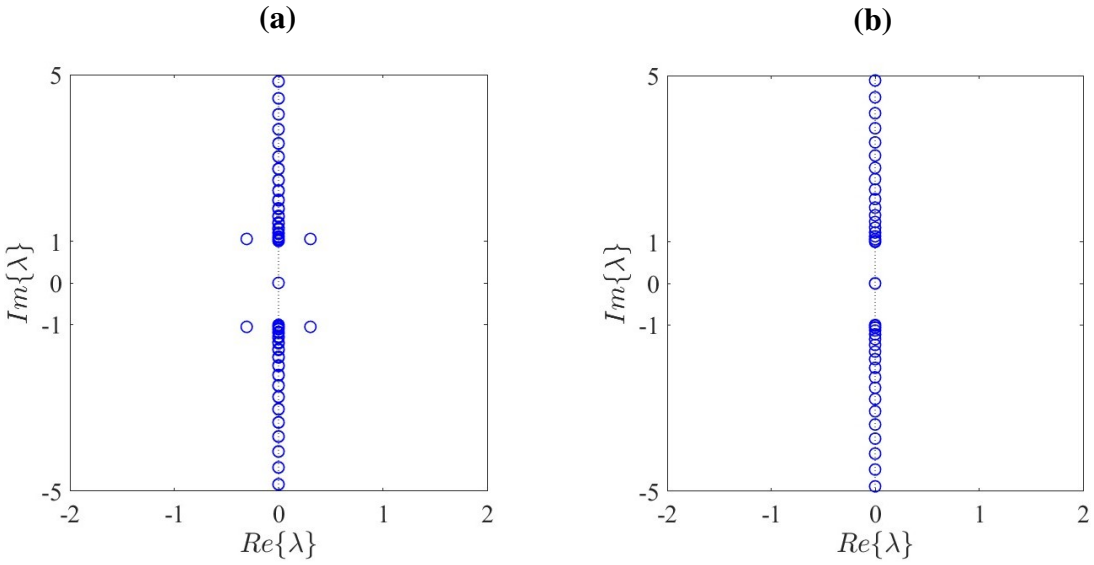

Figure 5.21 : Linear spectra of NLS equation for $\mu = 1$, $\Gamma = 0$ with a $\mathscr{P}\mathscr{T}$-symmetric potential; (a) $W_1 = 1.5, V_2 = 0.5$, (b) $W_1 = 1.5, V_2 = 2$

In Fig. 5.22, the momentum term coefficient Γ is increased to 0.1. In Fig. 5.22(a), for small potential depths, the system is observed to be linearly stable. With $\Gamma = 0.1$ and small potential depths, the soliton remains linearly stable, with no positive real parts in the eigenvalues. This shows that the system's stability is maintained, and choosing small potential values supports this stability.

However, in Fig. 5.22(b), when the complex potential depth is increased to $W_2 = 1.5$, the system becomes unstable, as seen in the nonlinear stability analysis. The soliton becomes linearly unstable, and eigenvalues with positive real parts appear. This result indicates that increasing the complex depth can destabilize the system, leading to both nonlinear and linear instability.

In Fig. 5.23, the same potential depths $W_1 = 0.5$ and $V_2 = 1.5$ are used, and the system is analyzed for $\Gamma = 0.1$ and $\Gamma = 0.2$. In Fig. 5.23(a), for $\Gamma = 0.1$, the system is observed to be linearly stable. The real potential depth is sufficient to stabilize the system, and no eigenvalues with positive real parts are found.

However, in Fig. 5.23(b), with a small increase in Γ to 0.2, the system becomes linearly unstable. Eigenvalues with positive real parts appear, indicating instability. This behavior is in good agreement with the nonlinear stability results, where increasing

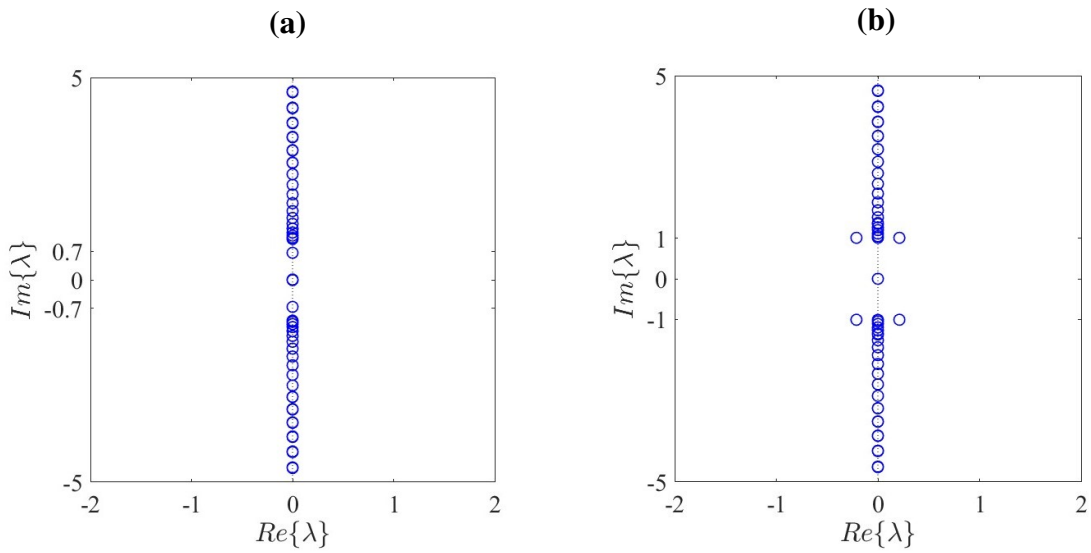

Figure 5.22 : Linear spectra of NLS equation for $\mu = 1, \Gamma = 0.1$ with a $\mathscr{P}\mathscr{T}$-symmetric potential; (a) $W_1 = 0.5, V_2 = 0.5$, (b) $W_1 = 1.5, V_2 = 0.5$

Γ also led to instability. The linear instability follows the same trend, showing that even small changes in Γ can destabilize the system.

This analysis highlights that while the real part of the potential can maintain stability up to a point, small increases in the momentum term Γ can disrupt the soliton's stability and lead to linear instability.

In Fig. 5.24, two different cases for the momentum term Γ are examined: $\Gamma = 0.2$ and $\Gamma = 0.4$. In Fig. 5.24(a), with $\Gamma = 0.2$, the complex depth of the potential W_1 is also increased. In this case, the soliton is found to be linearly unstable, with eigenvalues showing positive real parts. The increase in the potential depth and the value of Γ contributes to the soliton instability.

In Fig. 5.24(b), with $\Gamma = 0.4$, a significant number of eigenvalues have positive real parts, indicating that the system is linearly unstable. This higher value of Γ severely disrupts the system's stability, making the soliton linearly unstable.

Finally, in Fig. 5.25, the linear spectra of the NLS equation are studied for $\Gamma = -0.1$ and $\Gamma = -0.2$, under the conditions $W_1 = 0.5$ and $V_2 = 1.5$.

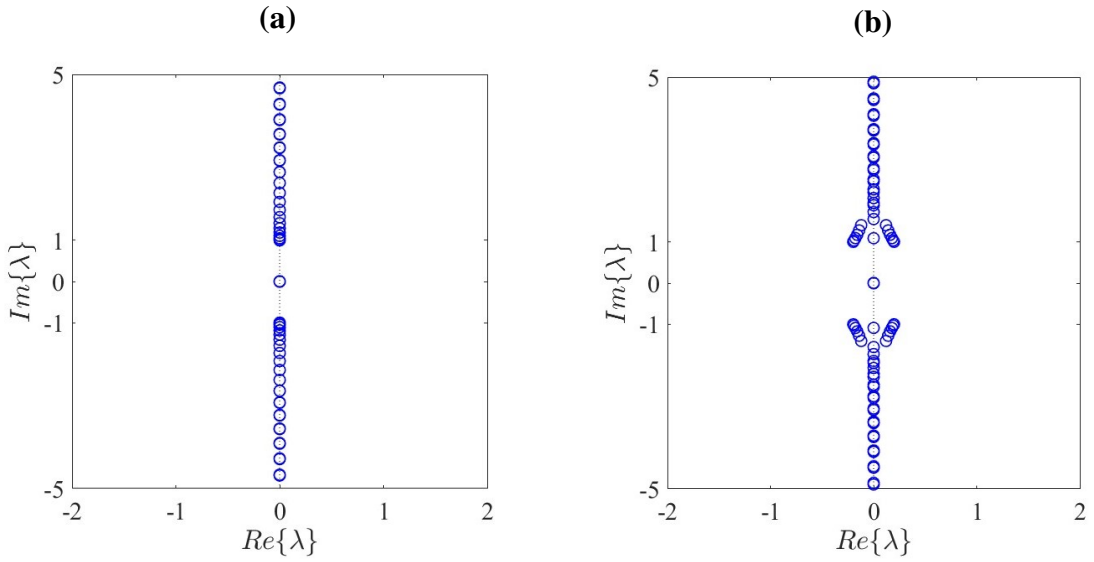

Figure 5.23 : Linear spectra of NLS equation for $\mu = 1, W_1 = 0.5, V_2 = 1.5$ with a $\mathscr{P}\mathscr{T}$-symmetric potential; (a) $\Gamma = 0.1$, (b) $\Gamma = 0.2$

In Fig. 5.25(a), for $\Gamma = -0.1$, the eigenvalues are observed to cluster along the imaginary axis, indicating linear stability. The spectral behavior in this case closely resembles that of the system with $\Gamma = 0.1$.

In Fig. 5.25(b), for $\Gamma = -0.2$, the eigenvalues maintain a similar distribution, with no real components present. This structure is similar to the spectral behavior for $\Gamma = 0.2$, further reinforcing the conclusion that the different signs of Γ has almost the same impact on the linear stability of the system.

Throughout the analyses, the effects of the momentum term Γ and the real and complex potential depths on the system's stability have been explored. For small Γ and low potential depths, the system is observed to be both nonlinearly and linearly stable. However, as the value of Γ increases, especially with larger complex potential depths, the soliton's stability deteriorates, and the system becomes both nonlinearly and linearly unstable. These results demonstrate the significant impact of the momentum term and potential parameters on the system's overall stability.

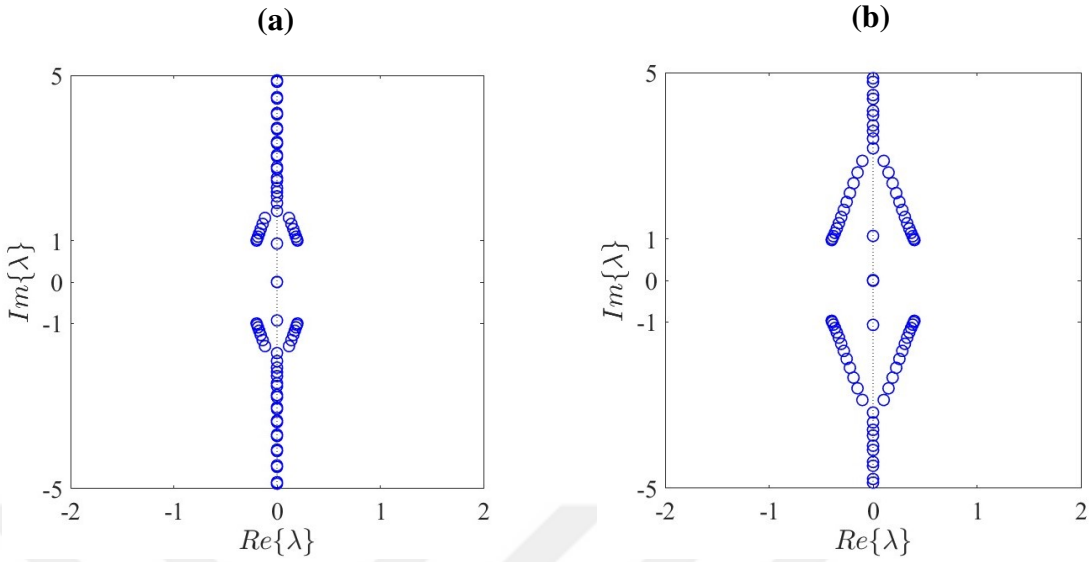

Figure 5.24 : Linear spectra of NLS equation for $\mu = 1$ with a $\mathscr{P}\mathscr{T}$-symmetric potential; (a) $\Gamma = 0.2$, $W_1 = 1.5, V_2 = 1.5$, (b) $\Gamma = 0.4$ $W_1 = 0.5, V_2 = 1$

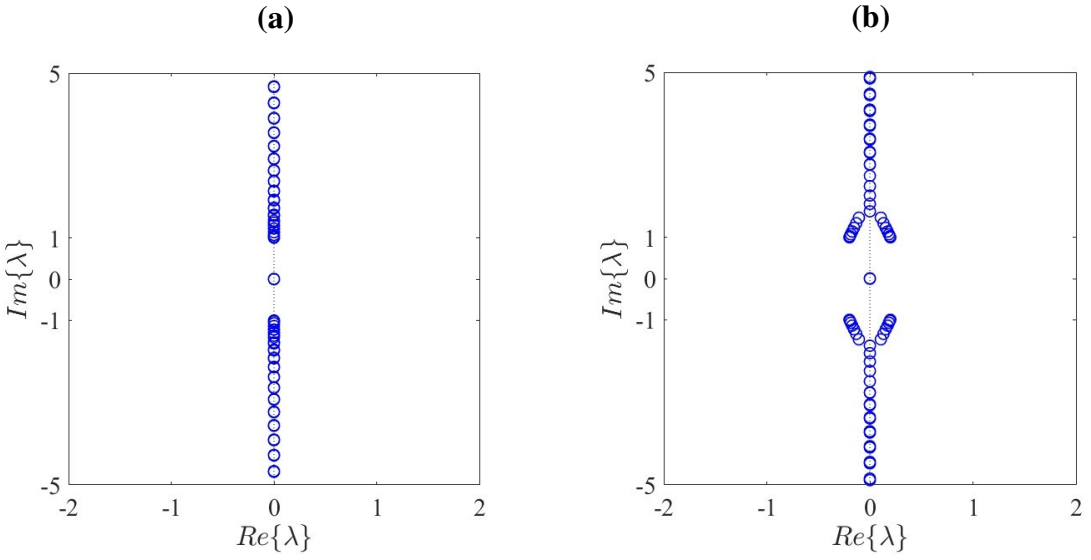

Figure 5.25 : Linear spectra of NLS equation for $\mu = 1$ with a $\mathscr{P}\mathscr{T}$-symmetric potential; (a) $\Gamma = -0.1$, $W_1 = 0.5, V_2 = 1.5$, (b) $\Gamma = -0.2$ $W_1 = 0.5, V_2 = 1.5$

6. CONCLUSION AND RECOMMENDATIONS

In this thesis, the NLS equation with a momentum term and an external $\mathscr{P}\mathscr{T}$-symmetric potential is investigated. Using SR Method, solitons of NLS equation with and without a momentum term and a $\mathscr{P}\mathscr{T}$-symmetric potential are obtained. How the coefficient of the momentum term, Γ, and the propagation constant, μ, affect stationary solitons in the absence of a $\mathscr{P}\mathscr{T}$-symmetric potential is examined, an it is concluded the amplitude of the solitons increase by increasing μ and they decrease by increasing Γ.

Additionally, by introducing ansatz and defining the structure of the $\mathscr{P}\mathscr{T}$-symmetric potential, exact solutions to this problem is established. The $\mathscr{P}\mathscr{T}$-symmetric potential is viewed as an extended form of the Scarf II potential.

A graphic comparing the two aforementioned solitons are shown to demonstrate the overlap between the analytical and numerical solutions. The numerical existence region for this model equation is plotted for a range of potential depths (V_2, W_1) and values of Γ. It is noted that the existence region is slightly decreased by the additional momentum term for the increasing coefficient Γ.

Additionally, Split-Step Fourier method is used to examine the resulting solitons' nonlinear stability features. The nonlinear stability cannot be achieved for the increasing momentum term values. The nonlinear stability properties of some particular solitons are presented and discussed with various figures for different potential depths. It is observed that for greater values of the real part of the potential chosen, the soliton becomes more stable and for greater values of the complex part of the potential chosen, it becomes unstable.

The linear stability characteristics of the obtained solitons are also investigated in the final section of this thesis by examining the linear spectrum. To illustrate the results, the linear spectra of the obtained solitons are plotted in some graphs. The conclusion

is that the linear stability of the obtained solitons are in good agreement with their properties.

In future studies, the momentum term, which is not deeply analyzed in the current literature, can be taken as a function of x instead of a constant, and a third or fourth order dispersion to the system can also be added. Additionally, quintic nonlinearity can be considered and computed cubic-quintic nonlinearity can also be investigated. The effects of various μ values can be investigated. Other types of external potentials can be used instead of the extension of Scarf II potential that is used in this thesis. Other modifications to address the collapses at higher values of Γ can also be explored. These steps aim to analyze the behavior of the momentum term's effect and different solitons of the modified NLS equation.

REFERENCES

[1] **Sulem, C. and Sulem, P.** (1999). The Nonlinear Schrödinger Equation: Self focusing and Wave Collapse, *New York: Springer*.

[2] **Ablowitz, M.** (2011). *Nonlinear Dispersive Waves Asymptotic Analysis and Solitons*, Cambridge University Press.

[3] **Kivshar, Y. and Agrawal, G.** (2003). *Optical Solitons: From Fibers to Photonic Crystals*, Academic Press, USA.

[4] **Ablowitz, M.**, **Prinari, B. and Trubatch, A.** (2003). *Discrete and Continuous Nonlinear Schrödinger Systems*, Cambridge University Press, USA.

[5] **Schneider, T.**, (2004). The Nonlinear Schrödinger Equation, Nonlinear Optics in Telecommunications, Advanced Texts in Physics, Springer, Berlin, Heidelberg, pp.119–142.

[6] **Petviashvili, V.** (1976). Equation of an extraordinary soliton, *Plasma Physics*, *2*, 469–472.

[7] **Kadomtsev, B. and Petviashvili, V.** (1970). On the Stability of Solitary Waves in Weakly Dispersing Media, *Soviet Physics—Doklady*, *15*, 539.

[8] **Ablowitz, M. and Musslimani, Z.** (2005). Spectral renormalization method for computing self-localized solutions to nonlinear systems, *Optics Letters*, *30*(16), 2140–2142.

[9] **Kartashov, Y.**, **Malomed, B. and Torner, L.** (2011). Solitons in nonlinear lattices, *Reviews of Modern Physics*, *83*, 247–306.

[10] **Bosshard, C.**, **Spreiter, R.**, **Zgonik, M. and Günther, P.** (1995). Kerr nonlinearity via cascaded optical rectication and the linear electro-optic effect, *Physical Review Letter*, *74*, 2816–2819.

[11] **Fibich, G. and Ilan, B.** (2000). Self-focusing of elliptic beams: an example for the failure of the aberrationless approximation, *Journal of the Optical Society of America*, *17*, 1749–1758.

[12] **Wazwaz, A.** (2006). Exact solutions for the fourth order nonlinear Schrodinger equations with cubic and power law nonlinearities, *Mathematical and Computer Modelling*, *43*, 802–808.

[13] **Kohl, R.**, **Biswas, A.**, **Milovic, D. and Zerrad, E.** (2008). Optical soliton perturbation in a non-Kerr law media, *Optics Laser Technology*, *40*, 647.

[14] **Lomdahl, P.** (1984). What is a soliton, *Los Alamos Science*.

[15] **Kartashov, Y.**, **Vysloukh, V. and Torner, L.** (2009). Soliton shape and mobility control in optical lattices, *Progress in Optics*, *52*, 63–148.

[16] **Musslimani, Z.**, **Makris, K.**, **El Ganainy, R. and Christodoulides, D.** (2008). Optical solitons in PT periodic potentials, *Physical Review Letters*, *100*(030402).

[17] **Musslimani, Z.**, **Makris, K.**, **El Ganainy, R. and Christodoulides, D.** (2008). Analytical solutions to a class of nonlinear Schrödinger equations with PT -like potentials, *Journal of Physics A: Mathematical and Theoretical*, *41*, 244019.

[18] **Makris, K.**, **El Ganainy, R.**, **Christodoulides, D. and Musslimani, Z.** (2011). PT -Symmetric Periodic Optical Potentials, *International Journal of Theoretical Physics*, *50*, 1019.

[19] **Yang, J.** (2015). Symmetry breaking of solitons in two-dimensional complex potentials, *Physical Review E*, *91*, 023201.

[20] **Yang, J.** (2014). Symmetry breaking of solitons in one-dimensional parity-time-symmetric optical potentials, *Optics Letters*, *39*, 5547.

[21] **He, Y.**, **Zhu, X.**, **Mihalache, D.**, **Liu, J. and Chen, Z.** (2012). Lattice solitons in PT -symmetric mixed linear-nonlinear optical lattices, *Physical Review A*, *85*(013831).

[22] **Göksel, I.**, **Antar, N. and Bakırtaş, I.** (2015). Solitons of (1+1)D cubic-quintic nonlinear Schrödinger equation with PT -symmetric potentials, *Optics Communications*, *354*, 277–285.

[23] **Göksel, I.**, **Antar, N. and Bakırtaş, I.** (2015). Nonlinear Lattice Solitons in Saturable Media, *Applied Mathematics and Information Sciences*, *1*, 377–385.

[24] **Göksel, I.**, **Antar, N. and Bakırtaş, I.** (2015). Two-dimensional solitons in cubic-saturable media with PT -symmetric lattices, *Chaos, Solitons Fractals*, *109*, 83–89.

[25] **He, Y.**, **Zhu, X.**, **Mihalache, D.**, **Liu, J. and Chen, Z.** (2012). Solitons in PT -symmetric optical lattices with spatially periodic modulation of nonlinearity, *Optics Communications*, *285*, 3320–3324.

[26] **Karlsson, M. and A., H.** (1994). Soliton-like pulses governed by fourth order dispersion in optical fibers, *Optics Communications*, *104*, 303.

[27] **Wazwaz, A. and Kaur, L.** (2019). Optical solitons for nonlinear Schrödinger (NLS) equation in normal dispersive regimes, *Optik*, *184*, 428–435.

[28] **Biswas, A.**, **Milovic, D.**, **Zerrad, E. and Majid, F.** (2006). Exact solutions for the cubic-quintic nonlinear Schrödinger equation, *Science Direct*, 958–964.

[29] **Triki, H. and Taha, T.** (2012). Solitary wave solutions for a higher order nonlinear Schrödinger equation, *Mathematics and Computers in Simulation*, *82*, 1333.

[30] **Meza, A.**, **Dutra, A.**, **Hott, M. and Roy, P.** (2015). Wide localized solutions of the parity-time symmetric nonautonomous nonlinear Schrödinger equation, *Physical Review E*, *91*(013205).

[31] **Cole, J. and Musslimani, Z.** (2014). Band gaps and lattice solitons for the higher-order nonlinear Schrödinger equation with a periodic potential, *Physical Review A*, *90*(013815).

[32] **Cole, J. and Musslimani, Z.** (2015). Spectral transverse instabilities and soliton dynamics in the higher-order multidimensional nonlinear Schrödinger equation, *Physica D: Nonlinear Phenomena*, *313*(26), 063807.

[33] **Yan, Z. and Chen, Y.** (2017). The nonlinear Schrödinger equation with generalized nonlinearities and PT -symmetric potentials: Stable solitons, interactions, and excitations, *Chaos: An Interdisciplinary Journal of Nonlinear Science*, *27*(7).

[34] **Bender, C. and Boettcher, S.** (1998). Real Spectra in Non-Hermitian Hamiltonians Having PT -Symmetry, *Physical Review Letters*, *80*, 5243.

[35] **Bender, C.** (2008). PT -symmetric quantum mechanics, *Journal of Mathematical Physics*, *40*, 2201.

[36] **Abdou, B.**, **Ndzana, F.**, **Tiofack, L. and Mohamadou, A.** (2021). Linear stability analysis and spatial solitons in the one-dimensional and the two-dimensional generalized nonlinear Schrodinger equation with third-order dispersion and PT-symmetric potentials, *The European Physical Journal D*.

[37] **Yan, Z.**, **Chen, Y. and Wen, Z.** (2016). On stable solitons and interactions of the generalized Gross-Pitaevskii equation with PT - and non-PT -symmetric potentials, *Chaos*, *26*(083109).

[38] **Chen, Y.**, **Yan, Z. and Li, X.** (2018). One- and two-dimensional gap solitons and dynamics in the PT-symmetric lattice potential and spatially-periodic momentum modulation, *Communications in Nonlinear Science and Numerical Simulation*, *55*, 287–297.

[39] **Bagci, B. and Quesne, C.** (2010). An update on PT -symmetric complexified Scarf II potential, spectral singularities and some remarks on the rationally-extended supersymmetric partners, *Journal of Physics A: Mathematical and Theoretical*, *43*(305301).

[40] **Yang, J.** (2010). Nonlinear waves in integrable and nonintegrable systems, *Siam*, 332–342.

[41] **Göksel, I.** (2017). Lattice Solitons in Cubic-Quintic Media, *Ph.D. thesis*, İstanbul Teknik Üniversitesi Institute of Science and Technology, Istanbul.

APPENDICES

APPENDIX A.1 : Fourier Transform

APPENDIX A.1

For a continuous, smooth, and absolutely integrable function $f(x)$, the integral transform

$$F(k_x) = \frac{1}{\sqrt{2\pi}} \int_{-\infty}^{\infty} f(x) e^{i(k_x)x} dx \tag{A.1}$$

is called the Fourier transform of $f(x)$, and conversely, the transform

$$F(k_x) = \frac{1}{\sqrt{2\pi}} \int_{-\infty}^{\infty} f(x) e^{-i(k_x)x} dx \tag{A.2}$$

is called the inverse Fourier transform of $F(k_x)$.

The Fourier transform of f is denoted by $\mathscr{F}(f) = \hat{f}$, and the inverse Fourier transform of $\hat{f}$ is denoted by $\mathscr{F}^{-1}(\hat{f})$, and clearly $\mathscr{F}^{-1}(\hat{f}) = \mathscr{F}^{-1}(\mathscr{F}(\hat{f}))$.

Integral transform methods are very useful for solving partial differential equations because of their properties such as linearity, shifting, scaling, etc.

Suppose that $f(x)$ tends to zero as x tends to infinity. Then,

$$\mathscr{F}(f'(x)) = ik_x \mathscr{F}(f(x)) \tag{A.3}$$

This result can be extended to obtain the differentiation property of the Fourier transform:

$$\mathscr{F}(f^n(x)) = (ik_x)^n (f(x)) = (ik_x)^n \hat{f}, n \in \mathbb{N} \tag{A.4}$$

CURRICULUM VITAE

Name Surname: Haldun Taha UZUNOĞLU

EDUCATION:

- **B.Sc.:** 2022, Istanbul Technical University, Faculty of Science and Letters, Mathematics Engineering
- **M.Sc.:** 2025, Istanbul Technical University, Graduate School, Department of Mathematics Engineering

PROFESSIONAL EXPERIENCE:

- **December 2022 - Present:** Research Assistant, Istanbul Technical University, Department of Mathematics Engineering, Sariyer/Istanbul

OTHER PUBLICATIONS, PRESENTATIONS AND PATENTS:

- **Uzunoğlu, H. T.**, Bakırtaş, İ. (2024). Solitons of NLS Equation with Momentum Term and a $\mathscr{PT}$-Symmetric Potential. *International Congress on Natural Sciences & Applied Mathematics*, June 07-08 2024, Istanbul, Türkiye